

Low Frequency Hybrid Instability In Quantum Magneto Semiconductor Plasmas

By

Aneesa Iqbal

Regn.#00000278189



A dissertation submitted in partial fulfillment of the requirements
for the degree of Master of Science in Physics

Supervised by

Dr. Muddasir Ali Shah

School of Natural Sciences (SNS)


National University of Sciences and Technology (NUST)

Islamabad, Pakistan

(2021)

National University of Sciences & Technology**MS THESIS WORK**

We hereby recommend that the dissertation prepared under our supervision by: Aneesa Iqbal, Regn No. 00000278189 Titled: Low Frequency Hybrid Instability In Quantum Magneto Semiconductor Plasmas accepted in partial fulfillment of the requirements for the award of **MS** degree.

Examination Committee Members1. Name: Dr. M. ALI PARACHASignature:  _____2. Name: DR. AEYSHA KHALIQUESignature:  _____External Examiner: DR. AZHAR HUSSAINSignature:  _____Supervisor's Name: DR. MUDDASIR ALI SHAHSignature:  _____



 Head of Department

22/02/2021

 Date

COUNTERSIGNEDDate: 28/2/2021



 Dean/Principal

Acknowledgements

I bow my head in deep gratitude to **ALMIGHTY ALLAH** who endowed me with potential and ability to the already existing ocean of knowledge and special praises to **Hazrat Muhammad** (PBUH).

This dissertation is the result of many people's dedication. Special mention goes to my supervisor, **Dr. Muddasir Ali Shah**. My experience in **MS** has been amazing and I thank him wholeheartedly, not only for his academic support, but also for his patience, motivation, and enthusiasm. Thanks to my GEC members **Dr. Muhammad Ali Paracha** and **Dr. Aeysha Khalique** for their encouragement.

Finally, my deepest gratitude goes to my loving **Parents, Brother** and **Sisters** who always prayed for my success. A heartfelt thanks for their help, encouragement, and support. This is my great pleasure to acknowledge the effort of those whose name may not appear on the cover.

ANEESA IQBAL

Abstract

The electrostatic low-frequency hybrid wave generated by the classical electron beam in electron-hole plasma is discussed here using the quantum hydrodynamic model (QHD). Semiconductors provide a suitable source to investigate such waves because of the mass asymmetry of electrons and holes which leads to charge separation and oscillating electric field in the electron-hole plasma. This oscillating electric field produces various electrostatic modes and drives instability in electron-hole plasma. Many quantum effects are considered such as quantum Bohm potential, perturbed Fermi pressure at $T > 0K$, exchange-correlation effects. To study the behavior of wave and instability growth rate, the derived dispersion relation is applied to GaAs compound semiconductor. The dynamics of the plasma species like electrons, holes, and beam electrons play an important role in the propagation and growth rate of the wave. Increasing the electron to hole number density causes a blue shift in the spectrum. The increase in electron beam speed will increase the instability whereas an increase in beam temperature will decrease the instability due to a larger amount of excited particles. Moreover if the angle between the LHW wavevector and the x-axis or the hole cyclotron frequency increases, the instability increases due to the stronger magnetic field.

Contents

1	An Introduction to Plasma	5
1.1	Plasma	5
1.2	Plasma in Nature	7
1.2.1	Ionosphere	7
1.2.2	Magnetosphere	8
1.3	Classical Plasma	10
1.4	Quantum Plasma	13
1.5	Degenerate Plasma	15
1.6	Semiconductor Plasma	18
1.7	Properties of semiconductors	20
1.7.1	Effective Mass	20
1.7.2	Electron Density (concentration) in Intrinsic and Extrinsic Semiconductors	22
1.8	Exchange-Correlation Effects	24
1.9	Dynamical Response of the Electron Gas	26
1.9.1	Dielectric Function from the Drude Model	27
1.9.2	Dielectric Function from the Lindhard Model	27
1.10	Instabilities in Semiconductors	29
2	Background	31
2.1	Maxwell's Equations	31

2.2	Waves in Plasma	35
2.2.1	Electromagnetic Waves	36
2.2.2	Electrostatic Waves	36
2.3	Electrostatic Modes in Semiconductor Plasma	37
2.3.1	Hole Acoustic Waves (HAWs)	37
2.3.2	Upper Hybrid Waves (UHWs)	38
2.3.3	Lower Hybrid Waves (LHWs)	39
2.4	Theoretical Descriptions to Study Behavior of Plasma	42
2.4.1	Single Particle Approach	42
2.4.2	The Kinetic Theory	43
2.4.3	The Fluid Theory	44
2.5	Pauli Blocking	47
3	Methodology	50
3.1	Quantum Hydrodynamic Model (QHM)	50
3.1.1	Bohm Potential	54
3.1.2	Fermi Pressure or Semi-Classical Pressure	55
3.2	Modeling of the Problem	61
3.2.1	Perturbed Velocity	62
3.2.2	Perturbed Number Density	69
3.2.3	Dielectric Response Function	72
3.2.4	Dispersion Relation	76
3.2.5	Analytical Study L.H.Ws in Quantum Semiconductor Plasma	77
4	Numerical Analysis and Discussion	82
5	Conclusion	90

List of Figures

1.1	States of Matter	5
1.2	Typical variation of neutral gas temperature and ionized gas density with various atmospheric layers	8
1.3	Head on crash between solar wind and Earths magnetosphere	9
1.4	Classification of plasma	12
1.5	Ideal Fermi gas at $T = 0\text{K}$ and $T > 0\text{K}$	16
1.6	Classification of materials	18
1.7	Curvature of charge carriers	19
1.8	(a) E and k relation of free particle. (b) E and k relation of particle in periodic potential.	21
1.9	Inverse of the second derivative of energy.	22
2.1	Lower hybrid electrostatic wave propagating at nearly perpendicular to unperturbed magnetic field B_0	40
2.2	Fermi-Dirac distribution function when $\frac{T}{T_F} < 1$	48
3.1	Fermi-Dirac distribution function	56
4.1	Typical parameters for different types of semiconductors.	83
4.2	Plot between $(\omega$ and $k)$ at $\omega_{ch} = 0.4$, $T_b = 0.4$, $T_h = T_e = 0.1$, $v_0 = 1$ and $\alpha = 0.6$. Dotted lines represent real part and Solid lines represent imaginary part at $\theta = 9^\circ, 10^\circ$	84

4.3	Plot between (ω and k) at $\omega_{ch} = 0.4, T_b = 0.4, T_h = T_e = 0.1, \theta = 10^\circ$ and $\alpha = 0.6$. Dotted lines represent real part and Solid lines represent imaginary part at $v_0 = 1, 1.5$ and 2	85
4.4	Plot between (ω and k) at $\omega_{ch} = 0.4, v_0 = 1, T_h = T_e = 0.1, \theta = 10^\circ$ and $\alpha = 0.6$. Dotted lines represent real part and Solid lines represent imaginary part at $T_b = 0.4, 0.6, 0.8$	86
4.5	Plot between (ω and k) at $T_b = 0.4, v_0 = 1, T_h = T_e = 0.1, \theta = 10^\circ$ and $\alpha = 0.6$. Dotted lines represent real part and Solid lines represent imaginary part at $\omega_{ch} = 0.4, 0.6, 0.8$	87
4.6	Plot between (ω and k) at $T_b = 0.4, v_0 = 1, T_h = T_e = 0.1, \theta = 10^\circ$ and $\omega_{ch} = 0.4$. Dotted lines represent real part and Solid lines represent imaginary part at $\alpha = 0.6, 0.7, 0.8, 0.9$	88
4.7	Plot between (ω and k) at $T_b = 0.4, v_0 = 1, \alpha = 0.6, \theta = 10^\circ$ and $\omega_{ch} = 0.4$. Dotted lines represent real part and Solid lines represent imaginary part at $T_h = T_e = 0.1, 0.3, 0.5$	89

Chapter 1

An Introduction to Plasma

1.1 Plasma

Plasma is one of the four states of matter alongside solid, liquid, and gas. The transition from one phase to another takes place by adding heat. As the temperature increases, the gas molecules collide with each other results in the detachment of a few electrons from the parent molecules and gas becomes ionized but not all ionized gases are plasma.

"Plasma by definition is a quasi-neutral gas of charged and neutral particles which exhibits collective behavior mediated by the electromagnetic forces"[1].

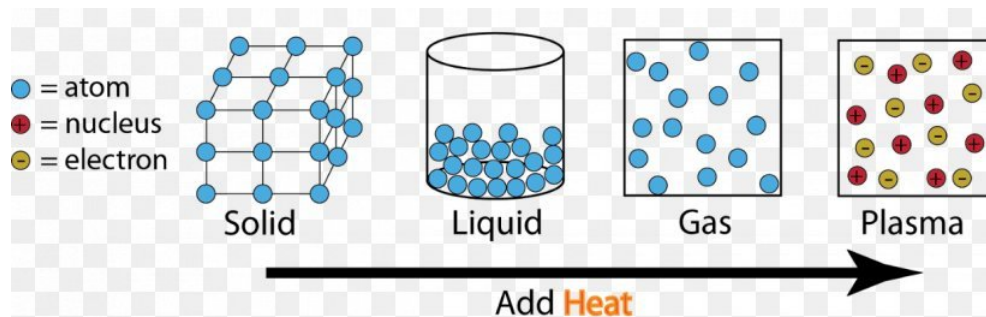


Figure 1.1: States of Matter

Here, the collective behavior represents a phenomenon specified by the whole ensemble of charged particles in the system. The charged particles in plasma at a distance beyond the Wigner-Seitz radius (the average particle separation distance $n^{1/3}$ in which n is the charged particle density), interact with many neighboring charged particles through their coulomb fields. This process is called collective interaction. The temperature and density are the most fundamental parameters of a plasma. High temperatures are usually required to maintain ionization. This energy is stored in different degrees of freedom of a plasma. But high temperature does not necessarily guarantee a plasma state. By decreasing the temperature the particles of the system become closer to each other. This reduces the degree of ionization as positive and negative charges combine to form atoms, and partially ionized plasma is formed. As the temperature is more decreased, the degree of ionization is so small that we are left with the system of the neutral gas.

In the low-temperature plasma, the electron temperatures are in the range of electron volts, which is sufficient for ionization, and the heavy species temperature is often close to room temperature. The degree of plasma ionization is determined by the Saha equation that relates the electron temperature to the ionization energy.

$$\frac{n_i}{n_n} \approx 2.4 \times 10^{21} \frac{T^{2/3}}{n_i} e^{\frac{-U_i}{k_B T}} \quad (1.1)$$

Here, n_i and n_n are respectively, the number density per m^3 of ionized atoms and neutral atoms, T is the gas temperature in kelvin, k_B is Boltzmann's constant and U_i is the ionization energy of the gas[2].

Along with the temperature, density is also a fundamental parameter of plasma. An incredible range of density can be seen in different systems as air and water differ in density by only 10^3 , while the density difference of water with white dwarf and

a neutron star is 10^5 and 10^{15} respectively. Table(1) shows a tremendous range of plasma densities and temperatures.

Table 1: Densities and temperatures of various plasma types

Type	Electron density	Temperature
	n_e (cm^{-3})	T_e (eV ^a)
Stars	10^{26}	2×10^3
Laser fusion	10^{25}	3×10^3
Magnetic fusion	10^{15}	10^3
Laser-produced	10^{18} – 10^{24}	10^2 – 10^3
Discharges	10^{12}	1–10
Ionosphere	10^6	0.1
Interstellar medium	1	10^{-2}

^a 1 eV \equiv 11 600 K.

1.2 Plasma in Nature

1.2.1 Ionosphere

A small portion of the Earth’s neutral atmosphere is ionized by solar ultraviolet (UV) radiation. These radiations ionize the oxygen molecules to create a positive ion and a free electron. At altitudes above 80 km collisions are too rare resulting in a low recombination rate of atmospheric particles and as a result, a permanent ionized population is formed called the ionosphere. The ionosphere extends to high altitudes 600 km and at low or mid-latitudes, it eventually merges into the plasmasphere. An atmospheric structure can be organized by temperature profile but the layer structure of the ionosphere is organized by the number density of the plasma. Initially, the temperature will decrease with altitude but at 10km altitude when the stratosphere begins it starts increasing because of UV absorption by ozone. Then at 50 km, it is maximum after that it will again decrease up to 90 km. Above a

region where there is a slight separation between the magnetosphere and solar wind known as magneto-pause, it increases drastically due to the high absorption of solar UV and EUV radiations. These radiations have enough energy to ionize the neutral atmosphere. Fig(1.2) shows the night and daytime profiles of solar radiation interaction with the atmosphere. During the daytime, these solar radiations are absorbed by the atmosphere and their intensity decreases in this process shown by the vertical layer in the figure. Most plasma densities occur in F-layer at noontime, because of high ionization rate of neutral gas results in high free electron concentration. Other layers(E, D) are formed by absorbing solar radiations of a different spectrum[3].

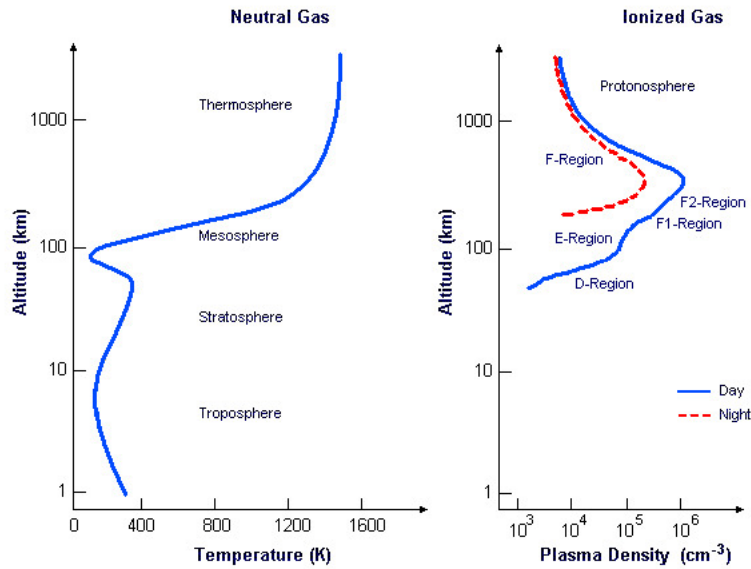


Figure 1.2: Typical variation of neutral gas temperature and ionized gas density with various atmospheric layers

1.2.2 Magnetosphere

A magnetosphere is an envelope of charged particles around a planet, where these charged particles are affected by that planet's magnetic field. The solar wind cannot

penetrate this magnetic field and deflect around it forming a comet-shaped bubble. The magnetosphere is stretched in a direction opposite to the sun, in such a way that a tail is formed known as magnetotail. The stretching of the magnetosphere is caused due to solar wind kinetic pressure, due to which the front side of the magnetosphere is compressed while the backside is stretched. Magnetosphere plasma mainly consists of electrons, protons, and a fraction of He^+ , O^+ ions, and He^{++} ions that come from the solar wind and ionization of particles in the ionosphere. The magnetosphere plasma is not evenly distributed but consists of different regions, each of which has a different temperature and densities. Magnetotail usually has a high density in the tail forming a thick plasma sheet. Average temperature and density in the sheet is $n_e \approx 0.5\text{cm}^{-3}$ and $T \approx 5 \times 10^6\text{K}$. The outer part of the tail has an density of $n_e \approx 10^{-2}\text{cm}^{-3}$ and temperature of $T \approx 5 \times 10^5\text{K}$ [4].

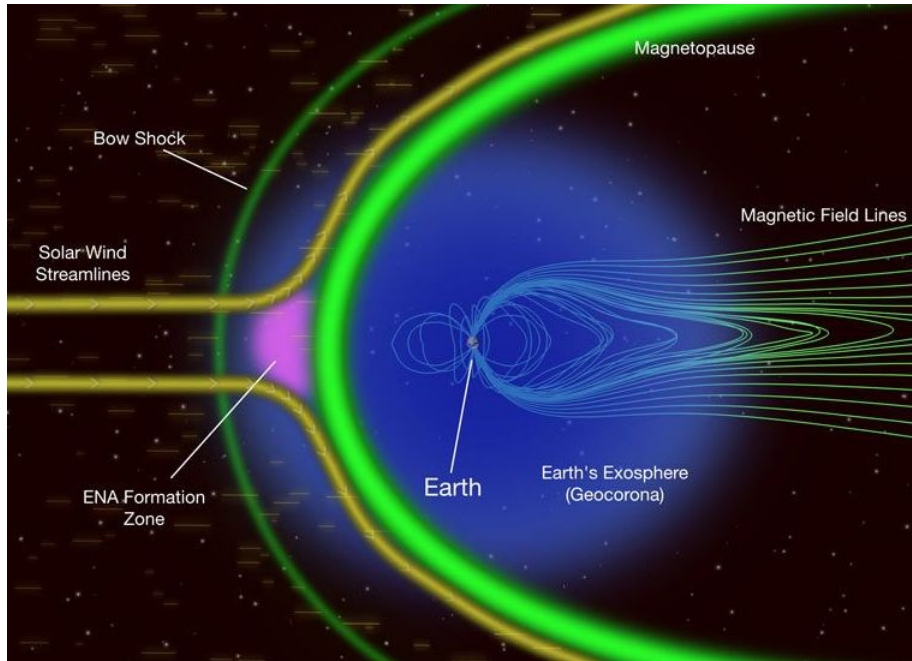


Figure 1.3: Head on crash between solar wind and Earths magnetosphere

1.3 Classical Plasma

In a classical plasma, the quantum mechanics have no significant role in the macroscopic dynamics of the plasma particles (except for the close inter-particle collisions which in general must be described quantum mechanically), such plasma is called classical plasma. In a classical plasma, the inter-particle distance is so large that the wave nature of charged particles plays no significant role in the collective properties of the plasma. Classical plasmas usually have a very high temperature and low density. Certain basic dimensionless parameters are used to describe this plasma regime. These parameters also help us in determining whether it is classical regime or quantum regime, and whether the individual effects (colloidal plasma) are dominants or collective effects (collision-less plasma) are dominants[5].

Thermal velocity

The thermal velocity of a plasma with finite temperature is defined as,

$$v_T = \left(\frac{2K_B T}{m}\right)^{1/2}. \quad (1.2)$$

This the thermal velocity of particles due to their random thermal motion, here k_B is the Boltzmann's constant, and m is the mass of particle.

Plasma frequency

The second parameter is plasma frequency which can be defined for a plasma system with number density n of the plasma particles, mass m , the electric permittivity because of Coulomb interaction, and electric charge e . With these parameters, we can construct a quantity known as plasma frequency that has the dimensions of an

inverse time and it is given as:

$$\omega_p = \left(\frac{e^2 n}{m \epsilon_0}\right)^{1/2} \quad (1.3)$$

where, "n" is the density of particles, ϵ_0 is the permittivity of free space. The plasma frequency is the characteristic oscillation frequency for electrons in a background of static positive ions that provide charge neutrality.

Debye Length

By combining the above two quantities, we can define a length scale known as the Debye length:

$$\lambda_D = \frac{v_T}{\omega_p} = \left(\frac{\epsilon_0 K_B T}{n e^2}\right)^{1/2}. \quad (1.4)$$

The Debye length describes an important phenomenon of electrostatic screening. If a test charge is placed in the plasma, a cloud of oppositely charged species will surround it. As a result, this test charge will be screened out and nearly become hidden from other particles situated at larger distances in plasma.

Coupling parameter

The coupling parameter is the ratio of mean interaction energy and kinetic energy of particles where mean interaction energy is given by,

$$U_{pot} = \frac{e^2 n^{1/3}}{\epsilon_0}, \quad (1.5)$$

and the kinetic energy is $k_B T$. Then the coupling parameter Γ_C can be written as:

$$\Gamma_C = \frac{U_{pot}}{K.E} = \frac{e^2 n^{1/3}}{\epsilon_0 k_B T} = 2.1 \times 10^{-4} \frac{n^{1/3}}{T}. \quad (1.6)$$

we can also write,

$$\Gamma_C = \left(\frac{1}{n\lambda_D^3}\right)^{\frac{2}{3}}. \quad (1.7)$$

From the above expression, it is clear that when the coupling parameter is small $\Gamma_C \leq 1$, the plasma is dominated by thermal effects, and Coulomb interactions are weak, which is known as the collision-less or weakly coupled plasma. On the contrary, when the coupling parameter is large $\Gamma_C \geq 1$, collisions become unavoidable and the plasma is said to be colloidal or strongly coupled. We also note that a classical plasma is collision-less at high temperatures and low densities[6].

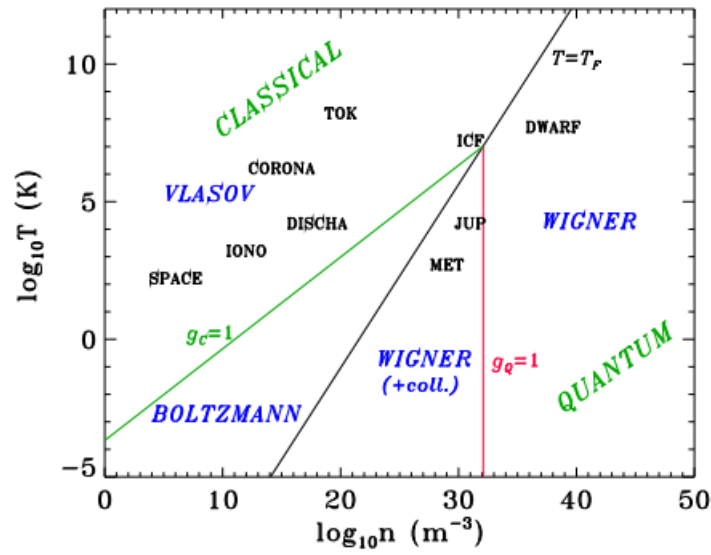


Figure 1.4: Classification of plasma

1.4 Quantum Plasma

Until the 1920s, plasma physics involves systems are highly dilute so that the QM effects were ignored. Sometimes for the systems that are so dense, quantum mechanics become necessary such as, in semiconductor quantum wells, semiconductor lasers, metallic systems, and nanoscale electronic devices. In such calculation, additional quantum mechanical results are plugged into completely classical frameworks. In a plasma system, when the mean inter-particle distance becomes comparable to the mean de-Broglie wavelength ($\lambda_B = \frac{h}{mv_T}$) of the lightest plasma particles and there is a significant overlap of particle wave functions due to quantum uncertainty, then this many-body problem is described by Fermi-Dirac statistics. In contrast to that, the usual laboratory and space plasma obey Maxwell-Boltzmann statistics. For classical regimes, the thermal de-Broglie wavelength that explains the spatial extension of the wave function is so small compared to the inter-particle distance that particles are considered as point-like. In this case, there is no wave functions overlapping and quantum interference. So on this basis, it is reasonable to say that quantum mechanical effects become important when the de Broglie wavelength becomes comparable or greater than Wigner-Seitz radius (the average inter-particle distance) $a = (\frac{3}{4\pi n})^{-\frac{1}{3}}$ [7].

$$\lambda_B \geq (\frac{3}{4\pi n})^{\frac{1}{3}} \implies \lambda_B \geq n^{-\frac{1}{3}}$$

Some important QM dimensionless parameters are given below.

Fermi velocity

In the QM regime, electrons are fermions that obey the Pauli exclusion principle that states that the same spin fermions cannot be placed in the same QM state. If our system has an N number of fermions in volume V, fermions with the same spin should not be placed in the same quantum state. Only fermions with the

opposite spin can be placed in the same quantum state. In this way, the fermions fill higher energy levels. This highest energy level is called the Fermi level and the corresponding energy is known as the Fermi energy E_F , which is given as:

$$E_F = \frac{\hbar^2 k_F^2}{2m}, \quad (1.8)$$

where k_F is length of Fermi sphere or Fermi wave vector,

$$k_F = (3\pi^2 n_0)^{1/3}, n_0 = \frac{N}{V} \quad (1.9)$$

Put this in equation (1.8) the Fermi energy will become,

$$E_F = \frac{\hbar^2}{2m} (3\pi^2 n_0)^{2/3}. \quad (1.10)$$

The Fermi velocity is given as,

$$v_F = \left(\frac{2E_F}{3m} \right)^{1/2}. \quad (1.11)$$

Fermi length

Now the ratio of plasma frequency and Fermi velocity gives us Thomas Fermi length or electrostatic screening length analogous to the Debye length,

$$\lambda_F = \frac{v_F}{\omega_p} = \left(\frac{2\epsilon_0 E_F}{3n_0 e^2} \right)^{1/2}. \quad (1.12)$$

Notice that if the system is at zero thermodynamic temperature, then $\lambda_D = 0$ while $\lambda_F \neq 0$. This is because at zero thermodynamic temperature in a classical system the electron gas cloud around the test charge will have no radii but for quantum electron gas Fermi sphere still exists.

Coupling parameter

The quantum coupling parameter is the ratio of the interaction energy U_{int} to the kinetic energy E_{kin} . The interaction energy or potential energy is the same as in the classical regime, whereas the kinetic energy is now given as the Fermi energy $E_{kin} = E_F$. So, coupling parameter is given as:

$$\Gamma_Q = \frac{U_{pot}}{K.E} = \frac{2me^2}{(3\pi^2)^{2/3}\epsilon_0 h^2 n_0^{1/3}} = 5.0 \times 10^{10} n_0^{-1/3}, \quad (1.13)$$

or

$$\Gamma_Q \approx \left(\frac{1}{n\lambda_F^3}\right)^{2/3}.$$

In a quantum collision-less regime, the quantum coupling parameter is small (E_{int} is small) and collective effects dominate. From the above expression, it is clear that a quantum plasma is more colloidal at higher densities, which is opposite to a classical plasma. This can be due to the Pauli exclusion principle, according to which two fermions cannot place in the same quantum state. At $T = 0\text{K}$ in a completely degenerate fermionic gas, all lower energy levels are filled. If we want to add more particles, we must supply enough energy to fill the high-energy levels. Therefore, increasing the number density of fermions will increase the Fermi energy of the fermionic gas[1][8].

1.5 Degenerate Plasma

Degenerate plasma is a highly dense and comparatively low-temperature plasma. These plasma are naturally found in the final stages of stars, such as white dwarfs and neutron stars. In these stars, thermal pressure is not enough to balance the gravitational pressure and to avoid gravitational collapse. Degenerate plasma parti-

cles are electrons, protons, neutrons, or other fermions (quarks and leptons). These plasma particles obey the Pauli exclusion principle. When the systems have low thermal energy the fermions will reside in low energy quantum states so all energy levels below the Fermi level are filled and above are empty. This is the full degeneracy state.

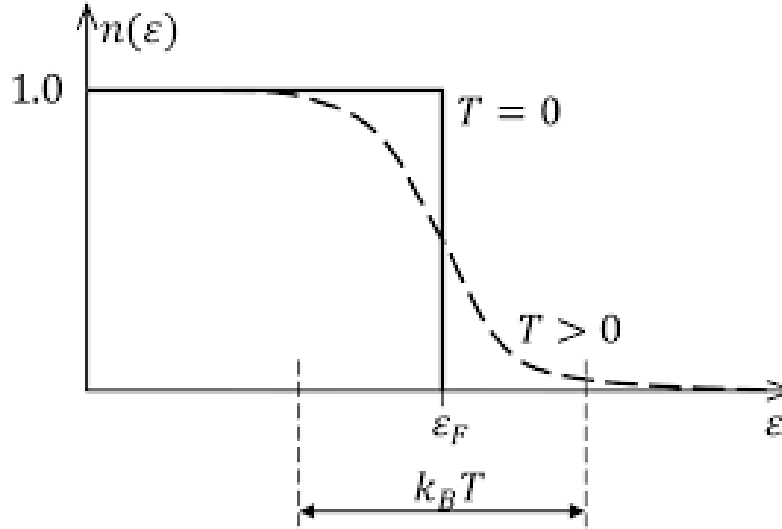


Figure 1.5: Ideal Fermi gas at $T = 0\text{K}$ and $T > 0\text{K}$

With the increase in temperature, the fermions occupy higher energy states as shown in fig (1.5), and plasma will become less degenerate. If plasma is cooled under increasing pressure after a certain limit further compression of the plasma becomes impossible. This limitation is due to the Pauli exclusion principle. In this highly compressed form, no extra space is available for the particle, thus particle's location is well define[9].

A low-density gas has a few electrons per cubic centimeter, free energy levels are available and electrons can easily reside there but in dense gas, this becomes impossible because the energy levels are filled. To move an electron to the available energy levels, a large amount of energy is required. In a degenerate plasma, most of the energy is absorbed by the nuclei moving very slowly except for a few electrons

to reach the top.

Another dimensionless parameter is degeneracy parameter $\chi = \frac{T_F}{T}$, that is Fermi temperature ($T_F = \frac{E_F}{k_B}$, where E_F is the energy of highest occupied energy level and k_B is the Boltzmann constant) to thermodynamic temperature ratio. Using the de-Broglie wavelength $\lambda_B = \frac{h}{(mv_T)}$, one can find the degeneracy parameter in the form of dimensionless parameter $n_0\lambda_B^3$ [7] as,

$$\chi = \frac{T_F}{T} = \frac{1}{2}(3\pi^2 n_0 \lambda_B^3)^{2/3}. \quad (1.14)$$

Therefore, if the mean inter-particle distance is comparable to the de Broglie wavelength, the Fermi Dirac statistics becomes necessary. So limitations on degeneracy parameter will identify whether plasma is degenerate or non-degenerate.

1) Non-Degenerate plasma:

$$\chi = \frac{T_F}{T} \ll 1 \implies T_F \ll T$$

2) Degenerate plasma

$$\chi = \frac{T_F}{T} \gg 1 \implies T_F \gg T$$

Low temperature and highly dense regimes take place in metals, semiconductors, nano-thin films at room temperature, and in astrophysical environments like in white dwarfs and neutron stars, where $T \approx 10^7 K$ and $T_F \approx 10^9 K$ so, the degenerate regime is achieved as $T_F \gg T \implies \chi = \frac{T_F}{T} \gg 1$ also, densities are high 10^{25}cm^{-3} .

1.6 Semiconductor Plasma

The atomic structure of a material is responsible for the electrical properties of a material, including conduction. An atom consists of a valence shell and a core with all the inner shells and the nucleus. In solids, the atoms are close enough that electronic orbitals tend to overlap. This intermixing leads to energy bands instead of a single energy level. Depending on the gap between the conduction band (completely or partially empty) and the valence band (completely or partially filled) materials are classified into three main groups: conductors, semiconductors, and insulators.

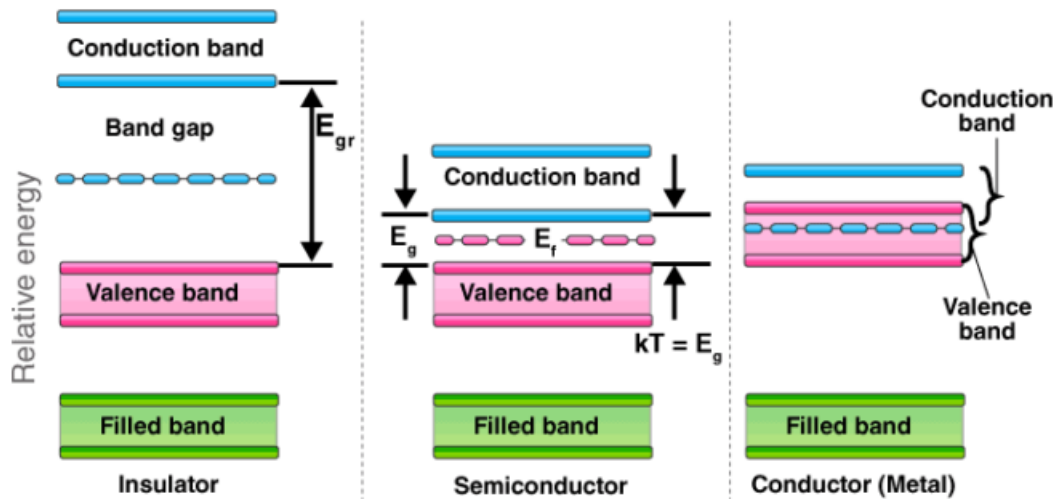


Figure 1.6: Classification of materials

Semiconductors are the materials in which the forbidden energy gap is small as shown in fig (1.6). They can conduct when the energy is supplied to charge carriers to overcome this energy gap E_g . When energy is pumped into a semiconductor, the electrons in the valence band get excited and jump to the conduction band leaving behind a hole in the valence band. These electrons with some higher energy now behave as if they are in a vacuum with different effective mass m^* . This process is known as electron-hole pair formation that satisfies plasma conditions.

Electrons and hole concentration can be controlled by doping (adding impurities

into the crystal structures. The number of charge carriers depends on doping. If there is an excess of holes in a semiconductor material it is named p-type otherwise with the excess of electrons, n-type. The dopants always rely on the atomic properties of both the dopant and the material to be doped.

Semiconductors are considered as one of the media which are compressed and low cost so they are used to study solid-state plasma in the quantum regime. The semiconductor quantum systems involve the electrons and holes in nano-scale such as (spintronics, nanotubes, Gunn oscillators, quantum wells, and quantum dots). The dimension of these systems becomes comparable or larger than the electron/hole thermal de-Broglie wavelengths. So, for sufficiently high electron/hole density and low temperature, it becomes essential to incorporate the quantum mechanical effects and study the dynamics of the electrons and holes under these effects. The quantum mechanical effects such as Bohm effect due to collective transport, exchange and correlation effects due to spin and Fermi pressures of degenerate quantum plasma particles play a crucial role in the collective behavior of the charge carriers in semiconductor electronic devices at nano scale[10][11].

In the semiconductors both electron and hole have different effective mass because of their different curvature in conduction and valence band.

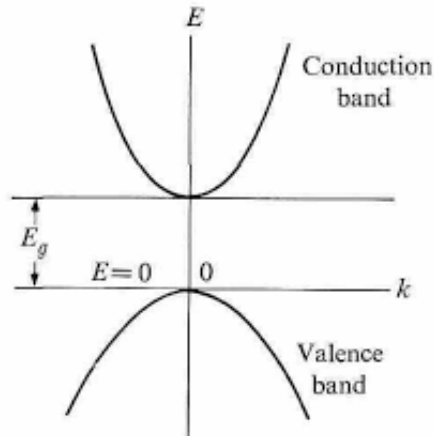


Figure 1.7: Curvature of charge carriers

This mass asymmetry creates charge separation and a restoring force will pull the charge carriers back to their equilibrium position but because of their inertia they will overshoot again a restoring force of opposite polarity will pull them backward. This results in the oscillation of charge carriers and this oscillation create waves or modes in plasma systems[12]. The investigation of these wave's stability or instability in electron-hole plasma has attracted considerable attention. The perturbation in the semiconductor quantum plasma can be created by using different sources such as electron beam pumping which initiates the instability. The electron beam interaction with the material generates electrons and holes, which satisfy our plasma conditions. The electron-hole oscillations excitation can be unstable and can grow in time[10][13].

1.7 Properties of semiconductors

1.7.1 Effective Mass

In solid-state physics when a material is subjected to some external potential such as (electric field, magnetic field, test charge, external pressure) the particles of that material move under the influence of this applied potential and periodic lattice potential of ions. Under the influence of such potential, the particles seem to have a mass different from that of true mass/rest mass. This mass is called effective mass[14]. As we know that free electron energy in a vacuum is given as:

$$E = \frac{\hbar^2 k^2}{2m}. \quad (1.15)$$

with m is the mass of electron. Now differentiate the above equation to get,

$$\frac{dE}{dk} = \frac{\hbar^2 k}{m} \implies \frac{d^2 E}{dk^2} = \frac{\hbar^2}{m}, \quad (1.16)$$

or we can write

$$m = \frac{h^2}{4\pi^2} \left(\frac{d^2 E}{dk^2} \right)^{-1}. \quad (1.17)$$

For the free electron model, the mass of electron remains constant so $\frac{d^2 E}{dk^2}$ is also constant. In this case, E versus k curve is parabolic as shown in fig (1.8a). But when the particles are under the influence of an external or internal potentials E and k curve is no longer parabolic. We experience different breakups in the parabolic curve which are the origin of allowed and forbidden gaps in materials as shown in fig (1.8b).

The mass given in the equation (1.18) is the effective mass which is represented by m^* and is equal to the inverse of the curvature of particle[15].

$$m^* = \frac{h^2}{4\pi^2} \left(\frac{d^2 E}{dk^2} \right)^{-1} \quad (1.18)$$

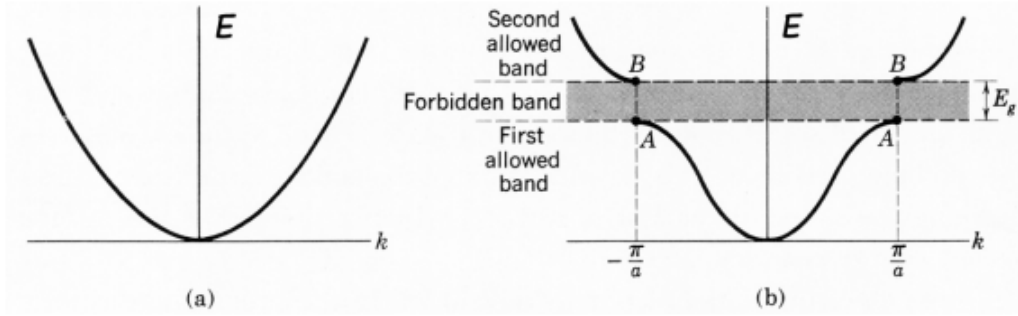


Figure 1.8: (a) E and k relation of free particle. (b) E and k relation of particle in periodic potential.

An important property of effective mass is that it can become negative near the Brillouin zone boundaries where first it reduce to zero and then become negative. Negative effective mass means particle curvature is opposite to the periodic poten-

tial. This also shows that particle curvature is no longer constant similar to mass and both are the functions of k as shown in fig (1.8).

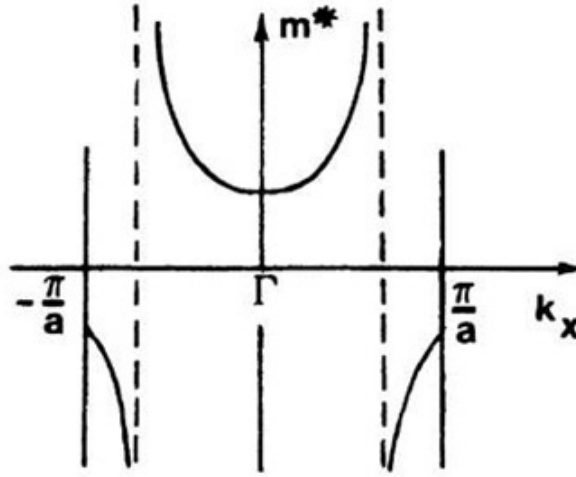


Figure 1.9: Inverse of the second derivative of energy.

From figure (1.9), it is clear that m^* is positive for small values of k (middle of Brillouin zone) and negative near the Brillouin zone boundaries at $k \approx \pm \frac{\pi}{a}$. It can only be equal to rest mass m_0 when energies do not lie near Brillouin zone boundaries, and the corresponding E/k curve is parabolic.

1.7.2 Electron Density (concentration) in Intrinsic and Extrinsic Semiconductors

Intrinsic Semiconductors:

These semiconductors are also called pure semiconductors e.g Ga, As, etc. At low values of temperatures, the valence electrons are attached to the atoms through covalent bonds. But when the temperature starts increasing thermal energy (KT) becomes comparable with the bond energy, some of the covalent bonds will start breaking, and electron-hole pairs will be generated[15].

$$n_e = 2 \left[\frac{2\pi m_e^* K T}{h^2} \right]^{3/2} e^{\frac{E_F - E_c}{K T}} \quad (1.19)$$

$$n_h = 2 \left[\frac{2\pi m_h^* K T}{h^2} \right]^{3/2} e^{\frac{E_v - E_F}{K T}} \quad (1.20)$$

where, n_e and n_h are the electron and hole concentration in intrinsic semiconductors. E_c and E_v are the conduction and valance band energies of semiconductor.

Extrinsic Semiconductors:

Extrinsic semiconductors are also called impure semiconductors or doped semiconductors. If the semiconductor is doped with an atom which has donor electron the semiconductor is called an n-type semiconductor and if the doped atom accept an electron then it is called a p-type semiconductor[15]. In n-type semiconductors, the electron and hole concentrations are given below

$$n_e = \frac{1}{2} [(N_D - N_A) + \sqrt{(N_D - N_A)^2 - 4n_i^2}], \quad (1.21)$$

and

$$n_h = \frac{n_i^2}{n_e}, \quad (1.22)$$

whereas in p-type semiconductors,

$$n_h = \frac{1}{2} [(N_D - N_A) + \sqrt{(N_D - N_A)^2 - 4n_i^2}], \quad (1.23)$$

and

$$n_e = \frac{n_i^2}{n_h}, \quad (1.24)$$

where, N_D and N_A are donor and acceptor concentrations[16].

1.8 Exchange-Correlation Effects

All the information about a system lies in its electronic structure. The quantum mechanical understanding of the electronic structure of a system requires dealing with a Schrodinger equation for N-body problems related to N-body wave functions given as:

$$\hat{H}\psi(x_1, x_2, x_3, \dots, x_N) = E\psi(x_1, x_2, x_3, \dots, x_N) \quad (1.25)$$

where,

$$\hat{H} = \sum_l \frac{P_l^2}{2M_l} + \frac{1}{2} \sum_{l \neq l'} \frac{q_l q_{l'}}{|\vec{R}_l - \vec{R}_{l'}|}$$

$$\hat{H}\psi = \sum_l \frac{P_l^2}{2M_l} \psi + \frac{1}{2} \sum_{l \neq l'} \frac{q_l q_{l'}}{|\vec{R}_l - \vec{R}_{l'}|} \psi = E\psi \quad (1.26)$$

In the above equation, the Hamiltonian operator contains all possible interactions. The first sum represents the kinetic energies of all electrons and nuclei. The second term represents the Coulomb attraction between the electrons and nuclei. M_l is the mass of all electrons and nuclei and q_l is the charge. From the computational point of view, it is an impractical task to solve the above equation, so different approximations are used to deal with this difficulty. The first approximation was suggested by Born and Oppenheimer in 1927 for the N-body problems. According to this approximation, the first step was to remove nuclei from the quantum mechanical problems and consider them fixed in space. Then solve the electronic problem without worrying about the nuclei. This approximation is mostly used in quantum chemistry for the computation of molecular wave functions of larger molecules. Unfortunately, Born Oppenheimer approximation becomes invalid when it is difficult to disentangle

the electrons and nuclei.

Further approximations to solve the above equation can be divided into two main categories based on the computational methods.

(i) Hartree and Hartree-Fock Theory

This is a wave function-based method. As Coulomb potential of an electron and a nucleus is responsible for all of the computational difficulty, so Hartree in 1928 suggested to replace this potential with an effective potential called electron-electron potential $U_{ee}(r)$. Effective potential means that each electron interacts with an average charge distribution due to all the other electrons. Such an effective potential is given as:

$$U_{ee}(\vec{r}) = \int d\vec{r}' \frac{e^2 n(\vec{r}')}{|\vec{r} - \vec{r}'|}, \quad (1.27)$$

where $n(\vec{r}) = \sum_j |\psi_j(\vec{r})|^2$ is the number density of electrons. The failure of the Hartree method is that it did not include the Pauli principle. The Hartree Wave function does not have the property to vanish when two same spin electrons occupy the same quantum state[17].

Fock and Slater (1930) showed that the way to include the Pauli principle is to work within the space of anti-symmetric wave functions. By assuming that the wave function can be approximated by a single Slater determinant made up of one spin-orbital per electron. The Hartree-Fock equation includes kinetic energy, Coulomb potential, and exchange potential. Exchange potential exists for the same spin electrons but vanishes for opposite spin electrons which are its limitation. As the true energy of the system is the sum of Hartree- Fock and correlation energy, so HF approximation failed to explain this correlation term.

$$E_{true} = E_{Hartree-Fock} + E_{correlation}$$

(ii) Density Functional Theory

DFT is a computational quantum mechanical method used to study the electronic structure (ground state) of N- body systems. DFT is one of the most successful and practical methods used in physics, chemistry, and material sciences. DFT gave the exact value of many-body wave functions but it involves some approximations. The foundation of DFT lies on two theorems of Hohenberg and Kohn (1964) and Kohn and Sham (1965)[18][19].

In 1964, Hohenberg and Kohn gave two theorems based on observations that ground electron number density contains the same information as wave-function of N electrons :

(a) The first theorem says that, if one knows the ground state of electrons then he can find an external potential from it. (b) The second theorem says that one can find a universal function of energy $E(n)$ in terms of density. Kohn and Sham (1965) modified DFT into a more practical approach that can be used for solving larger equations, also it involves exchange-correlation energy. Thomas Fermi theory is the first approximation to find the universal function of energy $E(n)$. Other approximations to find exchange-correlation energy from DFT are local density approximation (LDA) and generalized gradient approximation (GGA)[20][7].

1.9 Dynamical Response of the Electron Gas

In some solids, namely metals and doped semiconductors, some electrons are free and move throughout the material forming an electron gas and the ion core provides a uniform positive background. This electronic gas show response to outside influences like (test charges, electron beams, applied electric and magnetic fields, or an applied

pressure). Their response depends on electron's interactions with the ion core and with each other. The interaction of an electron with an ion core can be modeled by the idea of the effective mass and the interaction of electrons with each other can be explained by the dielectric function.

1.9.1 Dielectric Function from the Drude Model

Drude's model is a classical model used to describe the response of electronic gas in metals and doped semiconductors. This electron gas is not interacting with the positive ion background. The response of this electron gas to external potential, like time-dependent electric field $E = E_0 e^{-i\omega t}$, is given by the dielectric constant, given as:

$$\epsilon_L(\omega) = \epsilon_\infty - \frac{\omega_{pl}^2}{\omega^2 + i\gamma_D \omega}, \quad (1.28)$$

where ω_{pl} is the plasma frequency, ϵ_∞ is the dielectric contribution from the positive ion core and γ_D is the Drude model parameter[21].

1.9.2 Dielectric Function from the Lindhard Model

A quantum mechanical treatment for electron gas response to external potentials is done by Lindhard in 1954. This treatment is based on Random-Phase Approximation(RPA) and first-order perturbation theory. This method is capable of explaining screening at large and small wavelength limits[21]. The Lindhard dielectric function for an electron gas is given as:

$$\epsilon_L(q, \omega) = \epsilon_\infty - V_q \sum_k \frac{f(k+q) - f(k)}{E(k+q) - E(k) - \hbar(\omega + i\delta)}, \quad (1.29)$$

where $V_q = \frac{4\pi e^2}{q}$ is the Coulomb potential. $f(k)$ is the Fermi-Dirac distribution

function, $E(k)$ is the energy of an electron, δ is a positive infinitesimal constant, and the subscript L refers to Lindhard. This expression can be modified for different limited cases such as:

1) zero and large temperature limit 2) small and large wave vector limit 3) non-equilibrium distribution functions.

Case(1): For long wavelength or zero wave-vector limit $q = 0$ expression (1.29) has the same form as Drude dielectric constant[22]i.e;

$$\epsilon_L(\omega) = \epsilon_\infty - \frac{\omega_{pl}^2}{(\omega + i\gamma_L)^2}, \quad (1.30)$$

Case(2): For static potential or when the potential is varying slowly ($\omega + i\delta \approx 0$) and $\epsilon_\infty = 1$ equation (1.29) modified to Thomas Fermi screening dielectric constant, given as:

$$\epsilon(q) = 1 + \frac{q_F^2}{q^2} \quad (1.31)$$

where $q_F = \sqrt{\frac{4\pi e^2}{\epsilon} \frac{\partial n}{\partial \mu}}$ is the inverse Thomas Fermi length. For temperature $T = 0$, $n = \frac{1}{3\pi^2} \left(\frac{2m}{\hbar^2} E_F\right)^{3/2}$ and $\mu = E_F$, the Fermi wave vector will become,

$$q_F = \sqrt{\frac{6\pi e^2 n}{\epsilon E_F}}. \quad (1.32)$$

Thomas Fermi theory is valid only when the wave vector of wave packet must have the same length as the length of the first Brillouin zone i.e $q = q_F$. On the other hand, Lindhard theory is valid for all values of wave vector ($q \gg q_F$) even outside of 1st Brillouin zone. The value of Thomas Fermi length for metals and semiconductors are the order of one Angstrom that is the same as the typical inter-particle distance[23] [24][25].

1.10 Instabilities in Semiconductors

Semiconductors have various applications that require an understanding of the optical and electrical capabilities of semiconductors. Various researches have done work to find the safe and stable energy handling capabilities of semiconductors. This involves studying semiconductors under high energies to find what triggers the instabilities of charge carriers in semiconductors. The main outcome of these studies is that the main reason for semiconductor components breakdown is the formation of solid-state plasma because of the excitation of charge carriers to the conduction band. Solid-state plasma has a strong dependence on the bandgap of that specific semiconductor. Additional experiments using laser also prove the formation of plasma. Lasers produce an avalanche of electron gas that is highly absorptive, which leads to thermal failure in semiconductors. This process of heating is called Joule heating which increases the number of charge carriers and their kinetic energy. The concept of instabilities and equilibrium in solid-state plasma is mostly related to external potentials or confinement similar to interstellar plasma. These instabilities lead to a huge charge carrier population, change in current flow, and unstable dynamics of charge carriers. The solid-state plasma remains stable as long as there is constant free energy. When this free energy available for the carriers is increased using external injection such as electron beam, waves become excited leading to instabilities[26].

Instabilities are classified into four major categories depending on the driving force that initiate the instability.

Streaming Instabilities

When a current or an electron beam is driven through a plasma, various plasma species have different drift velocities. As a result, plasma waves can grow which can interact with the charge carriers and steal energy from the carriers resulting in

Landau damping.

Kinematic Instabilities

Kinematic instabilities are driven by temperature anisotropies or when the velocity distribution of plasma species is not Maxwellian. These types of instabilities are naturally seen in solar wind plasma[27].

Rayleigh-Taylor Instabilities

This type of instability is formed in plasma where the diffusive forces dominate. The most common example of these instabilities in solid-state plasma is the Gunn effect, which is the large fluctuation of current in semiconductors by applying high voltage. This effect is also used in forming Gunn diodes[28].

Universal Instabilities

The different ways in which a plasma is confined can lead to these instabilities. These instabilities also depend on the geometries of the material in which plasma is confined. If the solid-state plasma that is physically confined in a material expands rapidly, an increase in the free energy will lead to these instabilities[29].

Extraordinary safety measures must be taken to control these instabilities in a semiconductor. These often include a liquid nitrogen bath, application of quasi-steady state electric field, and magnetic field.

Chapter 2

Background

2.1 Maxwell's Equations

Maxwell's equations are originally a classical phenomenon but they explain the quantum mechanical phenomenon of photons in a semi-classical limit when the number of photons is large. This semi-classical phenomenon can be explained for semiconductors that undergo an interaction with an electron beam or light. The only drawback of this semi-classical phenomenon is that it fails to explain the spontaneous emission of light (lasers). There are two most common types of Maxwell's equations. (1) The first types are used to describe the interaction of electromagnetic radiation with matter. (2) The second type is used to describe the long-range interactions between charged particles in the form of conductivity. The second type of Maxwell's equations is of great importance in condensed matter physics, solid-state physics, and solid-state plasma because they explain the interaction of electromagnetic radiations with the matter as well as the interaction of electrons and phonons[30].

Maxwell's Equations in Vacuum

$$\nabla \cdot E = 4\pi\rho \tag{2.1}$$

$$\nabla \cdot B = 0 \quad (2.2)$$

$$\nabla \times E = -\frac{1}{c} \frac{\partial B}{\partial t} \quad (2.3)$$

$$\nabla \times B = \frac{1}{c} \frac{\partial E}{\partial t} + \frac{4\pi}{c} J \quad (2.4)$$

These are the Maxwell's equations in Gaussian units(cgs). Which are used for theoretical simplifications. These equations are also referred to as a microscopic set of equations in which the response of a material to the electromagnetic field is explicit. In the above equations, ρ and J represents the electric charge density and electric current density respectively, given as:

$$\rho = e(n_i - n_e), \quad (2.5)$$

$$J = e(n_i v_i - n_e v_e). \quad (2.6)$$

Here n_i and n_e are ion and electron number densities respectively. Equation (2.1) is the Gauss's Law that shows a relation between the static electric field and the electric charge density that is producing it. Equation (2.2) states that no magnetic mono-poles exists. Third Maxwell's equation is the Faraday's law which shows that a time-varying magnetic field is creating an electric field. Fourth Maxwell's equation is the Ampere's Law which states that the magnetic field can be produced in two ways i.e; by an electric current and by the time-varying electric field.

Maxwell's Equations In Medium

These Maxwell's equations are also called macroscopic Maxwell's equation in which the response of the system is incorporated in the microscopic equations. The most simple way to do that can be done in three steps.

Step 1

Step one is to separate the inside and outside charges (n_{int}, n_{ext}) and currents (J_{int}, J_{ext}) in the Maxwell's equations given above. Internal charges show a response to external charges.

Step 2

The equation of continuity is given as:

$$\frac{\partial \rho_{int}}{\partial t} + \nabla \cdot J_{int} = 0. \quad (2.7)$$

Taking integral on both side of equation (2.7)

$$\rho_{int} = -\nabla \cdot \int_0^t dt' j_{int}(t'), \quad (2.8)$$

or we can write,

$$\rho_{int} = -\nabla \cdot P, \quad (2.9)$$

where P is polarization (the electric dipole moment per-unit volume) given as:

$$P = \int_0^t dt' j_{int}(t'). \quad (2.10)$$

Step 3

Now as D is the dielectric displacement given as:

$$D = E + 4\pi P. \quad (2.11)$$

This shows the system's response to external electric field in the form of susceptibility $P_j = \sum_j \chi_j E_j$. Equation (2.11) will become,

$$D = E + 4\pi\chi E \implies D = \epsilon E \quad (2.12)$$

$$\epsilon = 1 + 4\pi\chi \quad (2.13)$$

Using equation (2.9) and (2.11) Maxwell's equations will become,

$$\nabla \cdot D = 4\pi\rho_{ext}, \quad (2.14)$$

$$\nabla \cdot B = 0, \quad (2.15)$$

$$\nabla \times E = -\frac{1}{c} \frac{\partial B}{\partial t}, \quad (2.16)$$

$$\nabla \times B = \frac{1}{c} \frac{\partial D}{\partial t} + \frac{4\pi}{c} J_{ext}. \quad (2.17)$$

The above equations represent Maxwell's equations in a medium, where ρ_{ext} and J_{ext} represents the external charge density and external current density respectively[15][31].

Now take the cross product of the Faraday's law,

$$\nabla \times (\nabla \times E) = -\frac{1}{c} \frac{\partial}{\partial t} (\nabla \times B), \quad (2.18)$$

Combining (2.17) and (2.18) we have,

$$\nabla \times (\nabla \times E) = -\frac{1}{c^2} \frac{\partial^2 D}{\partial t^2}, \quad (2.19)$$

use the value of the dielectric displacement from equation (2.12), to get

$$\nabla(\nabla \cdot E) - \nabla^2 E = -\frac{1}{c^2} \frac{\partial^2}{\partial t^2} (\epsilon E). \quad (2.20)$$

Now fourier transform this equation w.r.t space and time,

$$ik(ik \cdot E) - (ik)^2 E = -\frac{1}{c^2}(-i\omega)^2 \epsilon(k, \omega) E, \quad (2.21)$$

$$k^2 E - k(k \cdot E) = \frac{\omega^2}{c^2} \epsilon(k, \omega) E, \quad (2.22)$$

where, $\epsilon(k, \omega)$ is the dielectric tensor. It contains all the information about the linear properties of the system.

2.2 Waves in Plasma

Waves are the set of particles and fields that propagate in a periodic(repeating) manner. The important terms related to the waves in a plasma are given below.

Parallel and Perpendicular Propagating Waves

The propagation direction of wave vector k related to the unperturbed magnetic field classifies whether a wave is parallel or perpendicular propagating.

- (1) $k \parallel B_0$ condition for the parallel propagating wave which means the wave is traveling along the magnetic field.
- (2) $k \perp B_0$ condition for perpendicular propagating wave which means the wave is traveling across the magnetic field.

Transverse and Longitudinal Waves

The direction of wave vector w.r.t oscillating electric field decide whether a wave is longitudinal or transverse.

- (1) When $k \parallel E$ it is a longitudinal wave.
- (2) When $k \perp E$ it is a transverse wave.

Electromagnetic waves are mostly transverse and electrostatic waves are longitudinal. The further main classification of waves in plasma is based on an oscillating

magnetic field.

2.2.1 Electromagnetic Waves

Electromagnetic waves are transverse waves ($k \parallel E$) produced in a plasma but can also be partially longitudinal. In electromagnetic case the time varying magnetic field is non-zero $\frac{\partial B}{\partial t} \neq 0$ also $k \cdot E$ will vanish as $k \parallel E$.

So, Maxwell's equations in the electromagnetic case will reduce to the form

$$\nabla \cdot E = 0, \quad (2.23)$$

$$\nabla \cdot B = 0, \quad (2.24)$$

$$\nabla \times E = -\frac{1}{c} \frac{\partial B}{\partial t}, \quad (2.25)$$

and

$$\nabla \times B = \frac{1}{c} \frac{\partial E}{\partial t} + \frac{4\pi}{c} J. \quad (2.26)$$

For electromagnetic waves, equation (2.22) will also transform.

$$k^2 E = \frac{\omega^2}{c^2} \epsilon(k, \omega) E. \quad (2.27)$$

2.2.2 Electrostatic Waves

Electrostatic waves are longitudinal waves produced in plasma. They are produced due to perturbation either because of disturbance of internal electric neutrality or because of the externally applied field. These perturbations accelerate charged particles which result in plasma oscillations. These plasma oscillations can be produced by a local electron beam or a grid launcher excitation. Waves can further be divided into two modes based on oscillating species. (1) Electron modes (2) Ion modes.

Electron mode involves only electron dynamics due to the smaller mass of electrons whereas ions are assumed to be infinitely massive and static. An ion mode involves the dynamics of both species where ions are massive, and electrons are assumed to be massless. In electrostatic case, the time-varying magnetic field is zero i.e; $\frac{\partial B}{\partial t} = 0$. So, the Faraday' law becomes,

$$\nabla \times E = -\frac{1}{c} \frac{\partial B}{\partial t},$$

$$(\nabla \times E)_L = 0.$$

which means that the electric field associated with the electrostatic mode is curl free so it can be represented as a gradient of some scalar potential,

$$E = -\nabla\phi,$$

As in the electrostatic case, waves are longitudinal so $k \parallel E$ equation (2.22) will become

$$\frac{\omega^2}{c^2} \epsilon(k, \omega) E = 0 \tag{2.28}$$

$$\frac{\omega^2}{c^2} E \neq 0 \implies \epsilon(k, \omega) = 0 \tag{2.29}$$

2.3 Electrostatic Modes in Semiconductor Plasma

2.3.1 Hole Acoustic Waves (HAWs)

The low-frequency acoustic waves in plasma are the most fundamental electrostatic waves in which the wave vector is nearly perpendicular to the unperturbed magnetic field. Because of their simple mechanism, they have many applications in space and lab plasma including semiconductors. Primarily these waves develop by a small

charge separation that produces an electric field. These waves are also called Ion acoustic waves (IAWs) because the ion dynamics play an important role in wave propagation. In semiconductors, these waves are produced even without collisions because of the mass difference of electrons and holes and referred to as hole acoustic waves (HAWs). The final dispersion relation of hole acoustic waves excited by an electron beam in quantum semiconductor plasma is given as:

$$\omega^2 = v_{s,h}^2 k^2 + \frac{C_{s,h}^2 k^2 [v_0^2 - v_b^2] k^2}{(1 + \lambda_{s,Da}^2 k^2) [v_0^2 - v_b^2] k^2 - \omega_{pb}^2 \lambda_{s,Da}^2 k^2}, \quad (2.30)$$

where, $C_{s,h}^2 = \frac{\omega_{ph}^2}{\omega_{pe}^2} v_{s,e}^2$ is the effective sound speed with degenerate and quantum effects. $\lambda_{s,Da}^2 = \frac{v_{s,e}^2}{\omega_{pe}^2}$ is the modified form of Debye length[32]. By considering the electron beam oscillation frequency $\omega_{pb} = 0$. The above dispersion relation will modify to standard dispersion relation in quantum semiconductor plasma.

$$\omega^2 = v_{s,h}^2 k^2 + \frac{C_{s,h}^2 k^2}{(1 + \lambda_{s,Da}^2 k^2)}. \quad (2.31)$$

2.3.2 Upper Hybrid Waves (UHWs)

Upper hybrid waves are the electron electrostatic waves that propagate perpendicular to an unperturbed magnetic field. In this case, it is assumed that holes are fixed and form a uniform background. As the electron moves across the magnetic field two restoring forces act on these electrons. (1) Electric force (2) Lorentz force. The dispersion relation is given as[33]:

$$\omega^2 = \omega_{ce}^2 + v_{Fe}''^2 k_x^2 + \frac{\omega_{pe}^2 [v_0^2 - v_b^2] k_x^2}{[v_0^2 - v_b^2] k^2 - \omega_{pb}^2}, \quad (2.32)$$

In this equation, $v_{Fe}''^2$ is an effective velocity that contains all the thermal, quantum, and correlation effective. When the beam dynamics are not involved and all thermal,

quantum, and exchange-correlation effects are neglected, then the equation (2.32) will be modified to

$$\omega^2 = \omega_{ce}^2 + \omega_{pe}^2. \quad (2.33)$$

which is the classical non thermal upper hybrid wave dispersion relation.

2.3.3 Lower Hybrid Waves (LHWs)

Waves around the Lower hybrid wave (LHW) mode recently gain attention in different laboratory and space plasma environments such as in Tokamaks, fusion devices, and Earth's magnetopause because of their resonant interaction with both electrons and ions[34]. These waves have frequencies between the ion and electron gyro-frequencies $\omega_{ch} \ll \omega_{LH} \ll \omega_{ce}$ and with wavelengths between the electron and ion gyro radii. This allows LH waves to resonate with both species and transfer energy. This results in plasma heating or particle acceleration. The electrons with smaller Larmor radius are magnetized and can move only parallel to B , while the ions with larger Larmor radius are un-magnetized and free to move perpendicular to B . These waves mediate energy in between parallel and perpendicular motion of electrons and ions respectively[35][36].

Lower hybrid waves are nearly electrostatic with k vector nearly perpendicular to the magnetic field \vec{B} as shown in figure (2.1). In cold plasma, LH wave occurs at a frequency that is dependent on the angle between propagation wave vector \vec{k} and applied magnetic field \vec{B} .

$$\omega^2 = \omega_{LH}^2 \left(1 + \frac{m_i}{m_e} \cos^2 \theta\right), \quad (2.34)$$

where, m_i and m_e are masses of ions and electrons respectively and LH frequency is given as:

$$\omega_{LH} = \frac{1}{\sqrt{(1/\omega_{pi}^2 + 1/\omega_{ce}\omega_{ci})}}. \quad (2.35)$$

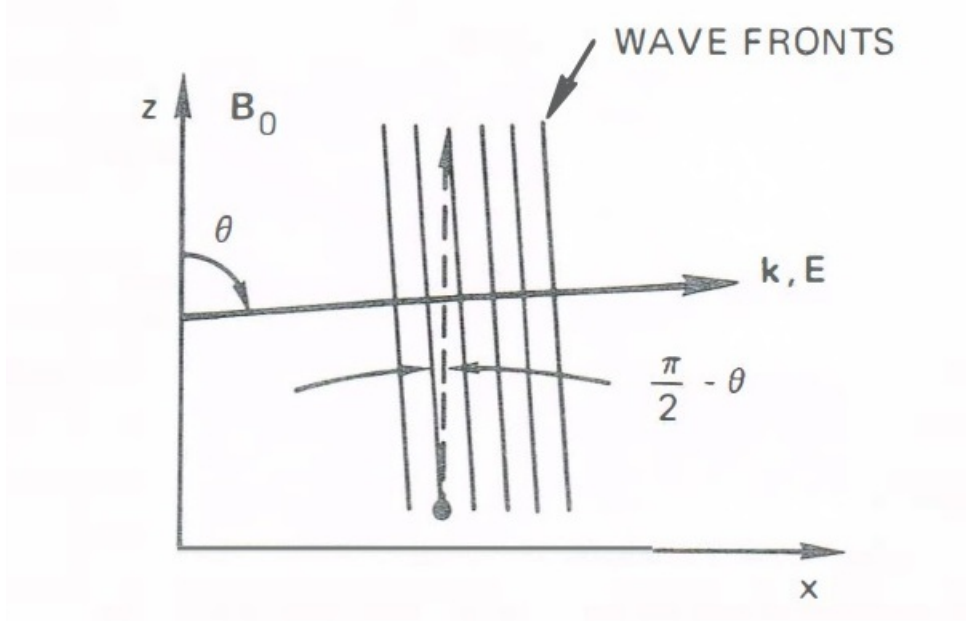


Figure 2.1: Lower hybrid electrostatic wave propagating at nearly perpendicular to unperturbed magnetic field B_0 .

In cold plasma when the wave is propagating at exact perpendicular to the unperturbed magnetic field ($k \perp B$) it can only resonate with the ions. Due to small Larmor radius ($r_L = \frac{m_e v_{\perp}}{eB}$) electrons cannot move along the x-direction and hardly oppose an electric field that moves them back and forth in the y-direction. However, if the electric field is not exactly perpendicular to B then the response time of ions will become less than or comparable to the response time of electrons, so now wave can resonate with both electrons and ions. For the LH resonance, the response time of ions should be smaller than or comparable to the response time of electrons. i.e.

when the following is satisfied.

$$\frac{m_i}{m_e} \cos^2 \theta \lesssim 1. \quad (2.36)$$

In warm plasma or when the electromagnetic effects are involved in plasma the LH resonance still satisfy the $\frac{m_i}{m_e} \cos^2 \theta \lesssim 1$ condition.

Hence, the parallel and perpendicular components of propagation wave vector k w.r.t B have different magnitude,

$$k_{\parallel}/k_{\perp} \lesssim \frac{m_e}{m_i} \ll 1$$

$$k_{\parallel} \ll k_{\perp}$$

The resonant condition of a lower hybrid wave for the un-magnetized ions is $\omega = kv_i$ and for the magnetized electrons is $\omega = k_{\parallel}v_{e\parallel}$. Thus LH waves interchange energy between ions and electrons as it moves perpendicular and parallel to the magnetic field either accelerate particles or heating them[37][38].

In a cold plasma system, the parallel distribution of electrons and perpendicular distribution of ions can generate LH waves. These waves then redistributing the energy among plasma species. Such redistribution can occur in the heliosphere, Earth's magnetotail, and solar corona. The wave damping and particle diffusion rates help us determine the redistribution of the non-thermal energy. To find these the phase ω/k and group speeds $\frac{d\omega}{dk}$, of the LH waves should be calculated. The dispersion relations for LH waves can be calculated either including electromagnetic (EM) effects by taking cold plasma regime or taking thermal plasma regime and electrostatic waves.

2.4 Theoretical Descriptions to Study Behavior of Plasma

Theoretically, different plasma models are used to study the behavior of plasma. This theoretical description involves solving simple Newton equations \implies fluid equations \implies kinetic equations. Choosing one or other theoretical methods depends on the problem at hand.

2.4.1 Single Particle Approach

As the most fundamental way to study the behavior of plasma is to study the behavior and trajectory of each particle under the influence of electromagnetic fields. This method is difficult from both theoretical and computational point of view. So, a simple way to overcome this difficulty is to study single/individual charged particles under the influence of electromagnetic fields.

The motion of these charged particles is given by Newton's equation of motion.

$$F = ma, \tag{2.37}$$

where $F = q(E + v \times B)$ is the Lorentz force, and $a = \frac{dv}{dt}$ is the acceleration. So above equation will become,

$$m \frac{dv}{dt} = q(E + v \times B). \tag{2.38}$$

The single-particle approach is mostly used to describe the gyration motion of particles, magnetic mirror effect, and adiabatic invariant of this cyclotron motion, etc. The single-particle approach is valid only when the charged particle density is low. This theoretical picture fails to explain the true plasma picture as plasma consists

of a large number of particles.

2.4.2 The Kinetic Theory

The kinetic theory describes plasma behavior on a microscopic level. In a kinetic approach, the statistical description of plasma particles is given by a six-dimensional distribution function $f(v, r, t)$ that contains all the information about plasma as a whole. This distribution function is different from a fluid picture where it only depends on (r and t).

Classical Kinetic Theory

The equation used in classical kinetic theory for this distribution function is the Vlasov equation given as:

$$\frac{\partial f}{\partial t} + v \cdot \frac{\partial f}{\partial r} - \frac{q}{m} \frac{\partial \phi}{\partial x} \cdot \frac{\partial f}{\partial v} = 0. \quad (2.39)$$

This equation is latter combines with the Maxwell's equations to find electric and magnetic fields and also with the Poisson equation to find electrostatic potential[39].

Quantum Kinetic Theory

The quantum mechanical kinetic description in phase space is given by Wigner function $f(r, v, t)$. For a quantum state, the Wigner function is given as:

$$f(r, v, t) = \frac{m}{2\pi\hbar} \int \exp\left(\frac{imvs}{\hbar}\right) \psi^*\left(x + \frac{s}{2}, t\right) \psi\left(x - \frac{s}{2}, t\right) ds \quad (2.40)$$

By using the Wigner function, we can find the macroscopic quantities like the number and current densities. This Wigner function obeys the Wigner equation given as:

$$\frac{\partial f}{\partial t} + v \cdot \frac{\partial f}{\partial x} - \frac{q}{m} \frac{\partial \phi}{\partial x} \cdot \frac{\partial f}{\partial v} = \frac{qh^2}{24m^3} \frac{\partial^3 \phi}{\partial x^3} \cdot \frac{\partial^3 f}{\partial v^3}. \quad (2.41)$$

From this equation, we can simply obtain the Vlasov equation by approximating $h \rightarrow 0$. The Wigner equation that describes the time evolution of the Wigner function can be coupled with the Poisson's equation to give,

$$\frac{\partial^2 \phi}{\partial x^2} = \frac{e}{\epsilon_0} \left(\int f dv - n_0 \right). \quad (2.42)$$

These Wigner-Poisson equations are used to describe the self-consistent collective electrostatic and electromagnetic field. This model has certain drawbacks. (a) This model is for collision-less and non-relativistic plasma. (b) Wigner - Poisson equation requires certain boundary conditions. In the case of bulk plasma systems (when size of the system is above 100nm) we can apply periodic boundary conditions but for nano-structures (1-100nm size). The size of the system is so small that it is difficult to choose suitable boundary conditions. (c) The Wigner function is non-localized and needs to be specified over whole space[6][5].

2.4.3 The Fluid Theory

The fluid theory describes the behavior of plasma on a macroscopic level. In the fluid model, the identity of individual particles is neglected and the dynamics of fluid elements are considered. The fluid theory is a reduced form of kinetic theory. The fluid theory is a localized description. One can find the macroscopic properties of the plasma system by taking the moments of Vlasov and Wigner equations. All of these moments satisfy fluid equations that do not involve any information about velocity space. In a classical fluid picture, the velocity distribution of all charged particles is considered to be Maxwellian everywhere and can be given by temperature T [8].

Classical multi-stream Model

According to Dawson, the classical analog of the Wigner distribution function can be written as:

$$f(x, v, t) = \sum_{\alpha=1}^N P_{\alpha} n_{\alpha}(x, t) \delta(v - u_{\alpha}(x, t)) \quad (2.43)$$

This is a distribution function for N- number of streams and it satisfy the Vlasov equation. Each fluid is characterized by their number density n_{α} , probability P_{α} and a velocity u_{α} , whereas δ represent the Dirac delta function. The velocity and number density given in equation (2.43) satisfy two-fluid equations.

$$\frac{\partial n_{\alpha}}{\partial t} + \frac{\partial}{\partial x}(n_{\alpha} u_{\alpha}) = 0 \quad (2.44)$$

$$\frac{\partial u_{\alpha}}{\partial t} + u_{\alpha} \frac{\partial u_{\alpha}}{\partial x} = \frac{e}{m} \frac{\partial \phi}{\partial x} \quad (2.45)$$

The main failure of the model is that when the velocity given in equation (2.43) is evolved in time, it has multiple values. This can cause a problem as when we calculate the density using the continuity equation it has infinite values at certain positions.

Quantum Fluid Models

Quantum mechanically the collective dynamic of N-number of charged particles can be explained by using Schrodinger equation for N- charged particles with corresponding wave function $\psi(x_1, x_2, \dots, x_N, t)$, but solving this problem is a difficult

task so, it is necessary to neglect certain effects by using zeroth-order approximation. In this approximation, higher-order correlation is neglected and the corresponding many body wave function split in product form[8].

$$\psi(x_1, x_2, \dots, x_N, t) = \psi_1(x_1, t), \psi_2(x_2, t), \dots, \psi_N(x_N, t)$$

This approximation also makes it clear that plasma is a collection of charged particles that interact through their collective field. There are two quantum fluid models. (i) The quantum analog of the multistream model (ii)The quantum hydrodynamic model. These models are based on Schrodinger's equation.

Schrodinger-Poisson Equation or Quantum Multistream Model

Schrodinger-Poisson equation is a system of an equation which is based on N-charged particle wave functions $\psi_\alpha(x, t)$.

$$ih \frac{\partial \psi_\alpha}{\partial t} = -\frac{\hbar^2}{2m} \frac{\partial^2 \psi_\alpha}{\partial x^2} - e\phi \psi_\alpha, \alpha = 1, 2, \dots, N \quad (2.46)$$

$$\frac{\partial^2 \phi}{\partial x^2} = \frac{e}{\epsilon_0} \left(\sum_{\alpha=1}^N P_\alpha |\psi_\alpha|^2 - n_0 \right) \quad (2.47)$$

In these equations, ϕ is the electrostatic potential. These equations do not involve spin and relativistic effects. For analytical, study we must introduce a wave function with A_α amplitude and S_α phase given as:

$$\psi_\alpha = A_\alpha e^{\frac{iS_\alpha}{\hbar}}. \quad (2.48)$$

Now the number density n_α and velocity u_α of α streams can be given as,

$$n_\alpha = |\psi_\alpha|^2 = A_\alpha^2, \quad (2.49)$$

$$u_\alpha = \frac{1}{m} \frac{\partial S_\alpha}{\partial x}. \quad (2.50)$$

Putting equation (2.48),(2.49) and (2.50) in (2.46) and (2.47) one can obtain the quantum multi-stream set of equations.

$$\frac{\partial n_\alpha}{\partial t} + \frac{\partial}{\partial x}(n_\alpha u_\alpha) = 0 \quad (2.51)$$

$$\frac{\partial u_\alpha}{\partial t} + u_\alpha \frac{\partial u_\alpha}{\partial x} = \frac{e}{m} \frac{\partial \phi}{\partial x} + \frac{\hbar^2}{2m} \frac{\partial}{\partial x} \left(\frac{\frac{\partial^2(\sqrt{n_\alpha})}{\partial x^2}}{\sqrt{n_\alpha}} \right) \quad (2.52)$$

From this equation, it is clear that if we put the limit $\hbar \rightarrow 0$ we are left with a classical multistream model. The advantage of the quantum multistream model is that it does not give infinite values of density. The wave will disperse due to quantum Bohm potential result into finite values of density[1][5][8].

2.5 Pauli Blocking

The concept of the Pauli exclusion principle is one of the most important and fundamental concepts in Quantum mechanics. It has a crucial rule in many branches of physics and chemistry including high-density plasma. The stability of high-density systems such as white dwarfs, neutron stars, is because of Pauli blocking. As we know that the coupling parameter of ordinary metals and semiconductors is greater than one so the collision of charged particles cannot be neglected. The quantum collisional regime is difficult to deal with since no collisional fluid model exists to deal with it except for the kinetic controversial Wigner (+ coll) model. Fortunately, the Pauli blocking effect helps us to reduce the collision rate drastically. If the system is at $T=0K$ all the energy states are filled and the collision rate is less. Even if the temperature is slightly above $0K$ the only electrons in the small $K_B T$ region

will undergo collisions as shown in figure (2.2).

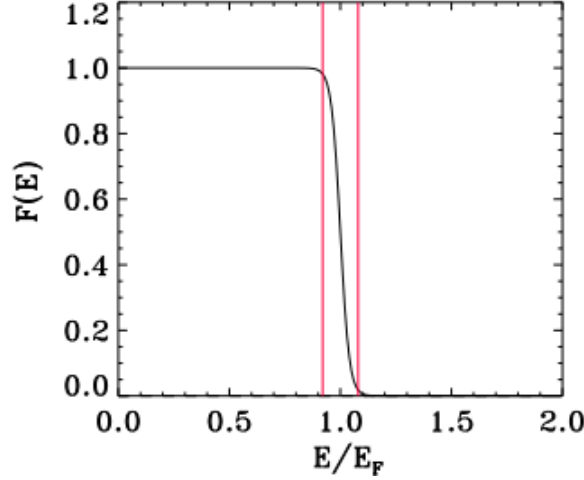


Figure 2.2: Fermi-Dirac distribution function when $\frac{T}{T_F} < 1$

For these slightly perturbed electrons the collision rate is given as:

$$v_{ee} \propto \frac{K_B T}{h}, \quad (2.53)$$

which is the inverse of collision time τ_{ee} . It can also be understood in the form of the uncertainty principle.

$$\Delta E \Delta t \approx h \quad (2.54)$$

The average collision rate can be calculated by multiplying equation (2.53) with the thickness of the region around the Fermi surface that is proportional to $\frac{T}{T_F}$ to get,

$$v_{ee} \approx \frac{K_B T^2}{h T_F}. \quad (2.55)$$

Above expression can be written in the form of coupling parameter as:

$$\frac{v_{ee}}{\omega_{pe}} \approx \frac{E_F}{h \omega_{pe}} \left(\frac{T}{T_F}\right)^2 \approx \frac{1}{g_Q^{1/2}} \left(\frac{T}{T_F}\right)^2. \quad (2.56)$$

So when $g_Q > 1$ then $v_{ee} < \omega_{pe}$ also $T < T_F$. As in the case of GaAs, for the electron temperature at $T = 2K$, Fermi temperature $T_F = 83.3K$ the corresponding coupling parameter is greater than one. The collisional time scale for this case will be

$$\tau_{ee} = 1.6 \times 10^{-10} \text{s}.$$

This electron-electron collision time is greater than the typical plasma collision-less time scale $\tau_p = \frac{2\pi}{\omega_{pe}} = 1.33 \times 10^{-13} \text{s}$. So it is evident that for the time scale smaller than τ_{ee} we can neglect collisions. This allows us to use collision-less models for this time scale. This effect will only work if the system is at absolute thermodynamic equilibrium or a slightly perturbed system. Because when the system is way beyond thermodynamic equilibrium we can not neglect collisions like in laser-induced plasma systems in semiconductors and metals the e-e collisions become unavoidable[40][41].

Chapter 3

Methodology

In this chapter, the first step is to choose an appropriate model for our problem. Many different types of models can be used for an N-body problem. Since we are interested in finding the response of quantum electron and hole gas to beam-induced perturbation in localized distribution. A suitable method for this case would be the Quantum hydrodynamic model (QHM).

3.1 Quantum Hydrodynamic Model (QHM)

Hydrodynamic models were formed in condensed-matter physics. In condensed-matter physics, these models are usually called time-dependent Thomas-Fermi models that are mainly used for the systems like electron gas in metal and semiconductors. Recently, these hydrodynamic models are used in gaseous quantum plasma such as the dense plasma system in cosmological objects like white dwarfs, neutron stars, and inertial confinement fusion.

The Quantum hydrodynamic model(QHD) can be developed by taking moments of the Wigner six-dimensional distribution function $f(x, v, t)$. The moment of order s is given below:

$$M_s(x, t) = \int_{-\infty}^{\infty} f(x, v, t) v^s dv. \quad (3.1)$$

Low-order moments gave us much needed physical quantities like the number density, velocity, and pressure. Each of these quantities satisfies certain fluid equations. The zeroth moment is the particle number density and it obeys the corresponding continuity equation. The first moment is the velocity and the corresponding fluid equation is the momentum equation (Euler equation). The second moment defines the pressure, and so on. Thus the equation for the n th-order moment requires the knowledge of the $(i+1)$ moment. This process generates an infinite number of fluid equations, but in the electrostatic case, moments up to 2nd order are enough. To close the system to a particular order a closure equation is required. This closure equation is the thermodynamic equation of state, like in the poly-tropic relation $P \propto n^\gamma$ the pressure and density relation[8].

The QHD model consists of the first three moments of the Wigner function $f(x, v, t)$, such as the number density given as:

$$n(x, t) = \sum_{\alpha=1}^N p_\alpha n_\alpha, \quad (3.2)$$

and the velocity is given as:

$$u(x, t) = \sum_{\alpha=1}^N p_\alpha \frac{n_\alpha}{n} u_\alpha. \quad (3.3)$$

These moments satisfy two set of equations, continuity equation and the Euler equation,

$$\frac{\partial n}{\partial t} + \frac{\partial(nu)}{\partial x} = 0, \quad (3.4)$$

$$\frac{\partial u}{\partial t} + u \frac{\partial u}{\partial x} = \frac{e}{m} \frac{\partial \phi}{\partial x} - \frac{1}{mn} \frac{\partial P}{\partial x}. \quad (3.5)$$

These equations seem to be similar to the classical system of equations obtained by taking the moments of the Vlasov equation. But in this case, the quantum nature is hidden in pressure terms. The pressure given in the above equation is the sum of classical and quantum mechanical pressure.

$$P = P^{cl} + P^Q \quad (3.6)$$

So, equation (3.5) can be written as:

$$\frac{\partial u}{\partial t} + u \frac{\partial u}{\partial x} = \frac{e}{m} \frac{\partial \phi}{\partial x} - \frac{1}{mn} \frac{\partial P^{cl}}{\partial x} - \frac{1}{mn} \frac{\partial P^Q}{\partial x} \quad (3.7)$$

These two pressures are given as:

$$P^{cl} = mn \left(\frac{\sum_{\alpha=1}^N p_{\alpha} n_{\alpha} u_{\alpha}^2}{n} - \frac{\sum_{\alpha=1}^N p_{\alpha} n_{\alpha} u_{\alpha}}{n} \right) \implies P^{cl} = mn (\langle v_{\alpha}^2 \rangle - \langle v_{\alpha} \rangle^2) \quad (3.8)$$

$$P^Q = \frac{\hbar^2}{2m} \frac{\partial}{\partial x} \sum_{\alpha=1}^N p_{\alpha} n_{\alpha} \left(\frac{\partial_x \sqrt{n_{\alpha}}}{\sqrt{n_{\alpha}}} \right) \quad (3.9)$$

Two assumptions are used on P^{cl} and P^Q to close the system.

(1) According to the first assumption, the amplitudes of all wavefunctions of plasma particles are the same. Also the spatial distribution of density $n_{\alpha} = |\psi_{\alpha}|^2$ will be equal to density n of all plasma particles. After applying this assumption the quantum pressure will become,

$$P^Q = \frac{\hbar^2 n}{2m} \left(\frac{\partial_x \sqrt{n}}{\sqrt{n}} \right). \quad (3.10)$$

(2) The second assumption involves considering an equation of state. This equation relates the electron density n to the classical pressure in the Euler equation,

$$P = P_0 \left(\frac{n}{n_0} \right)^\gamma. \quad (3.11)$$

That is a poly-tropic equation with exponent $\gamma = 3$ for 1D

$$P = \frac{mv_F^2}{3n_0^2} n^3. \quad (3.12)$$

where $P_0 = \frac{2}{3}n_0 E_F$ is the pressure at zero T .

The final form of QHD equation will be given as:

$$\frac{\partial n}{\partial t} + \frac{\partial(nu)}{\partial x} = 0 \quad (3.13)$$

$$\frac{\partial u}{\partial t} + u \frac{\partial u}{\partial x} = \frac{e}{m} \frac{\partial \phi}{\partial x} + \frac{\hbar^2}{2m^2} \frac{\partial}{\partial x} \left(\frac{\partial_x^2 \sqrt{n}}{\sqrt{n}} \right) - \frac{1}{mn} \frac{\partial P}{\partial x} \quad (3.14)$$

where m and e are the mass of electron and magnitude of the charge respectively [19]. The QHD model is derived from the Wigner-Poisson equations. The difference between the quantum multi-stream model and the QHD model is that in the Quantum hydrodynamic model the system of N stream equations is modified to only two sets of equations. This model still has certain drawbacks which are given below :

- (a) Quantum term are considered up to 2nd order in the Planck's constant.
- (b) This model can be used for the systems with wavelengths larger than the Thomas-Fermi screening length.

The latter limitation is similar to the classical fluid models, which are suitable for wavelength larger than the Debye length.[42].

3.1.1 Bohm Potential

The term in equation (3.14) that is proportional to \hbar^2 is a quantum mechanical correction to the classical fluid model referred to as Bohm potential. This potential is the main concept of deBroglie- Bohm's description of quantum mechanics. This is referred to as potential instead of quantum pressure because physically it explains the concepts of quantum tunneling and quantum uncertainty (wave packet spreading), so from a thermodynamics point of view, it is not pressure[1][43]. The Bohm potential can be described in the form of Fermi pressure of nano-metric objects given as

$$V_{Bohm} = \frac{\hbar^2}{2m} \left(\frac{\partial_x^2 \sqrt{n}}{\sqrt{n}} \right) \quad (3.15)$$

From Hamilton-Jacobi equation we can find quantum Bohm term in the form of wave length[44].

$$V_{Bohm} \approx \frac{\hbar^2}{m\lambda^2} \quad (3.16)$$

Also we know that the Fermi pressure at $T = 0K$ is given as:

$$P \approx nE_F \implies \frac{P}{E_F} \approx n \quad (3.17)$$

Now assume that the length scale given in equation (3.16) is approximately equal to Thomas-Fermi length $\lambda \approx \lambda_F$. Put value of $\lambda_F = \frac{v_F}{\omega_p}$ from equation (1.12) in Equation (3.16) we get,

$$V_{Bohm} \approx \frac{\hbar^2}{m\lambda_F^2} \approx \left(\frac{\hbar\omega_p}{mv_F} \right)^2 \quad (3.18)$$

Also,

$$\frac{V_{Bohm}}{E_F} \approx \left(\frac{\hbar\omega_p}{E_F} \right)^2 \quad (3.19)$$

Comparing equation (3.17) and (3.19) shows that Bohm potential has same impact as Fermi pressure[19].

3.1.2 Fermi Pressure or Semi-Classical Pressure

The semi-classical pressure given in equation (3.14) is the thermodynamic Fermi pressure. The concept of Fermi degenerate pressure can be understood in the form of wave particle duality of fermions. Since these fermions are confined to dense region like in white dwarfs, neutron stars or in metals and semiconductors. If we treat them as wave then the wavelength of these fermions will reduce so as to confine them to a smaller volume. This will increase the energy of fermions and collisions with other particles will also increase which give rise to Fermi degenerate pressure. This concept can also be explained by uncertainty principle which is given as,

$$\Delta x \Delta p \geq \frac{h}{2}.$$

Since the fermions position become certain by containing them to smaller volume the corresponding momentum become uncertain and will correspond to Fermi pressure. This pressure can be derived for full or partially degenerate gas.

Zero Temperature Properties of Fermi gas

Since electrons have half-integral so they are fermions and obey the Pauli exclusion Principle. At $T = 0$ all the low-energy states are filled up to a certain maximum energy level E_F . This state depends on the density of the Fermi gas and is called Fermi energy. The total number of fermions in a quantum level is given by the distribution function. For the fermions, this distribution function is Fermi-Dirac distribution. The Fermi-Dirac distribution gives the average number of the particles in the quantum level of energy ϵ and chemical potential μ given as:

$$f(\epsilon) = \frac{1}{e^{\beta(\epsilon-\mu)} + 1} \quad (3.20)$$

At $T = 0K$,

$$f(\epsilon) = 1, \text{ if } \epsilon < \epsilon_F$$

$$f(\epsilon) = 0, \text{ if } \epsilon > \epsilon_F$$

At $T = 0K$ the energy states start filling at the lowest level (ground energy level) and ϵ_F the highest occupied level. The states above ϵ_F are empty. So the states above ϵ_F are empty and below are filled. For a 3D system of free fermions the

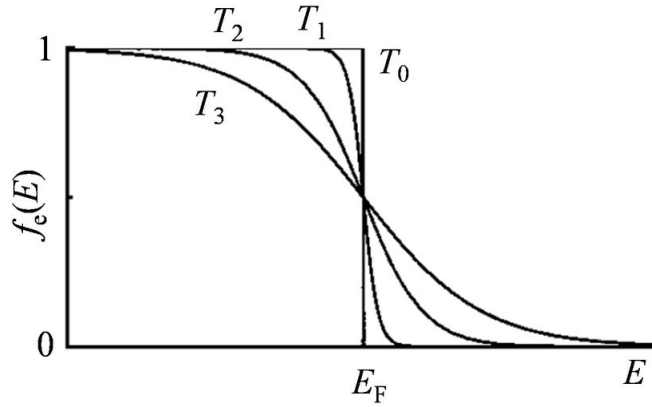


Figure 3.1: Fermi-Dirac distribution function

density of states $D(\epsilon)$ is given as:

$$D(\epsilon) = \frac{V}{2\pi^2 h^3} (2m)^{\frac{2}{3}} \sqrt{\epsilon}. \quad (3.21)$$

The Fermi pressure is given by,

$$P = -\left(\frac{U}{V}\right)_{T,\mu} \quad (3.22)$$

where, U is internal energy and V is the volume. At zero thermodynamic temperature the internal energy is given by,

$$U = \int_0^{\epsilon_F} \epsilon D(\epsilon) d\epsilon \quad (3.23)$$

Put eq (3.21) in eq (3.23) and integrate to get,

$$U = \frac{2}{5} \frac{V}{2\pi^2 h^3} (2m)^{\frac{2}{3}} \epsilon_F^{\frac{5}{3}}. \quad (3.24)$$

Pressure at $T = 0K$ will become,

$$P = \frac{2}{5} n \epsilon_F, \quad (3.25)$$

where ϵ_F is the Fermi energy in 3D given as:

$$\because \epsilon_F = \frac{3}{2} m v_F^2 = \frac{3h^2}{2m} (3\pi^2)^{\frac{2}{3}} n^{\frac{2}{3}}$$

$$\because v_F^2 = \frac{h^2}{m^2} (3\pi^2)^{\frac{2}{3}} n^{\frac{2}{3}}$$

$$P = \frac{3}{5} n m v_F^2 = \frac{3h^2}{5m} (3\pi^2)^{\frac{2}{3}} n^{\frac{5}{3}} \quad (3D) \quad (3.26)$$

$$P = \frac{1}{5} n m v_F^2 = \frac{h^2}{5m} (3\pi^2)^{\frac{2}{3}} n^{\frac{5}{3}} \quad (1D) \quad (3.27)$$

This is the Fermi pressure for Fermi gas at $T = 0K$ with the Fermi velocity $v_F = \sqrt{\frac{2E_F}{3m}}$. The pressure in equation (3.25) is for the whole system of particles, but when only " $\frac{1}{6}$ " of the particles are included the Fermi pressure will become,

$$P = n m v_F^2 \quad (3D) \quad (3.28)$$

$$P = \frac{1}{3} n m v_F^2 \quad (1D) \quad (3.29)$$

Non-Zero (low) Temperatures of Fermi gas

To find non- zero thermodynamic properties of indistinguishable particles like fermions, the statistical description is given in the form of canonical ensemble.

Step one is to introduce the grand partition function, Z_{gr}^{F-D} for fermions with two-fold degeneracy given as:

$$Z_{gr}^{F-D} = \prod_k^{\infty} (1 + \exp \beta(\mu - \epsilon_k)). \quad (3.30)$$

Thermodynamic properties of Fermi-Dirac systems are determined from the grand potential with two-fold degeneracy Ω_{gr}^{F-D} given as:

$$\Omega_{gr}^{F-D} = -\frac{2}{\beta} \ln Z_{gr}^{F-D}, \quad (3.31)$$

put equation (3.30) in (3.31) to get,

$$\Omega_{gr}^{F-D} = -\frac{2}{\beta} \prod_k^{\infty} \ln (1 + \exp \beta(\mu - \epsilon_k)) \quad (3.32)$$

as we know that pressure is given by,

$$P = -\left(\frac{\partial \Omega}{\partial V}\right)_{T,N}. \quad (3.33)$$

now put equation (3.32) in equation (3.33) to get,

$$P = \left[\frac{\partial}{\partial V} \frac{2}{\beta} \prod_k^{\infty} \ln (1 + \exp \beta(\mu - \epsilon_k))\right]_{T,N}, \quad (3.34)$$

$$P = \frac{2}{\beta} \prod_k^{\infty} \frac{\partial \ln (1 + \exp \beta(\mu - \epsilon_k))}{\partial V}, \quad (3.35)$$

$$P = \frac{2}{\beta} \prod_k \frac{\exp \beta(\mu - \epsilon_k)}{(1 + \exp \beta(\mu - \epsilon_k))} \left(-\beta \frac{\partial \epsilon_k}{\partial V} \right), \quad (3.36)$$

$$P = - \prod_k \frac{2}{(\exp \beta(\epsilon_k - \mu) + 1)} \left(\frac{\partial \epsilon_k}{\partial V} \right). \quad (3.37)$$

$$\because \epsilon_k = \frac{h}{2m} \left(3\pi^2 \frac{N}{V} \right)^{\frac{2}{3}}.$$

$$\frac{\partial \epsilon_k}{\partial V} = \frac{\partial}{\partial V} \left[\frac{h}{2m} \left(3\pi^2 \frac{N}{V} \right)^{\frac{2}{3}} \right],$$

$$\frac{\partial \epsilon_k}{\partial V} = \frac{2h}{6m} \left(3\pi^2 N \right)^{\frac{2}{3}} \left(-\frac{1}{V^{\frac{5}{3}}} \right),$$

$$\frac{\partial \epsilon_k}{\partial V} = -\frac{2}{3} \frac{\epsilon_k}{V}.$$

change the sum in equation (3.37) into integral over density of states and put value of ϵ_k to get,

$$P = \frac{4}{3V} \int_{-\infty}^{\infty} D(\epsilon_k) \frac{\epsilon_k}{(\exp \beta(\epsilon_k - \mu) + 1)} d\epsilon_k, \quad (3.38)$$

$$\because D(\epsilon_k) = \frac{V}{4\pi^2} \left(\frac{2m}{h} \right)^{\frac{3}{2}} \sqrt{\epsilon_k}.$$

$$P = \frac{1}{3\pi^2} \left(\frac{2m}{h} \right)^{\frac{3}{2}} \int_{-\infty}^{\infty} \frac{\epsilon_k^{\frac{3}{2}}}{(\exp \beta(\epsilon_k - \mu) + 1)} d\epsilon_k. \quad (3.39)$$

the integral in above equation can be solved by using Sommerfeld expansion given as:

$$\int_{-\infty}^{\infty} H(\epsilon)f(\epsilon)d\epsilon = \int_{-\infty}^{\mu} H(\epsilon)d\epsilon + \frac{\pi^2}{6\beta^2} \frac{d}{d\epsilon} H(\epsilon)|_{\epsilon=\mu} + O\beta^4 + \dots \quad (3.40)$$

The lower limit in 1st integral on R.H.S can be taken as zero because our lower energy state is zeroth state. This integral is given as:

$$\int_0^{\mu} H(\epsilon)d\epsilon = \int_0^{\epsilon_F} H(\epsilon)d\epsilon + (\mu - \epsilon_F)H(\epsilon_F). \quad (3.41)$$

eq (3.40) will become,

$$\int_{-\infty}^{\infty} H(\epsilon)f(\epsilon)d\epsilon = \int_0^{\epsilon_F} H(\epsilon)d\epsilon + (\mu - \epsilon_F)H(\epsilon_F) + \frac{\pi^2}{6\beta^2} \frac{d}{d\epsilon} H(\epsilon)|_{\epsilon=\epsilon_F} + O\beta^4 + \dots \quad (3.42)$$

eq (3.39) will become,

$$P = \frac{1}{3\pi^2} \left(\frac{2m}{h}\right)^{\frac{3}{2}} \left[\int_0^{\epsilon_F} \epsilon_k^{\frac{3}{2}} d\epsilon_k + (\mu - \epsilon_F)\epsilon_F^{\frac{3}{2}} + \frac{\pi^2}{6\beta^2} \frac{d}{d\epsilon_K} H(\epsilon)|_{\epsilon_K=\epsilon_F} \right] \quad (3.43)$$

$$P = \frac{1}{3\pi^2} \left(\frac{2m}{h}\right)^{\frac{3}{2}} \left[\frac{2}{5}\epsilon_F^{\frac{5}{2}} + (\mu - \epsilon_F)\epsilon_F^{\frac{3}{2}} + \frac{\pi^2}{4\beta^2}\epsilon_F^{\frac{1}{2}} \right], \quad (3.44)$$

chemical potential in 3D is given as:

$$\therefore \mu = \epsilon_F + \frac{\pi^2}{12\epsilon_F\beta}.$$

we get,

$$P = \frac{1}{3\pi^2} \left(\frac{2m}{h}\right)^{\frac{3}{2}} \left[\frac{2}{5}\epsilon_F^{\frac{5}{2}} + \left(-\frac{\pi^2}{12\epsilon_F\beta^2}\right)\epsilon_F^{\frac{3}{2}} + \frac{\pi^2}{4\beta^2}\epsilon_F^{\frac{1}{2}} \right], \quad (3.45)$$

$$P = \frac{1}{3\pi^2} \left(\frac{2m}{h}\right)^{\frac{3}{2}} \frac{2}{5}\epsilon_F^{\frac{5}{2}} \left[1 - \frac{5\pi^2}{24\beta^2\epsilon_F^2} + \frac{5\pi^2}{8\beta^2\epsilon_F^2} \right], \quad (3.46)$$

$$P = \frac{1}{3\pi^2} \left(\frac{2m}{h}\right)^{\frac{3}{2}} \frac{2}{5} \epsilon_F^{\frac{5}{2}} \left[1 + \frac{5\pi^2}{12\beta^2 \epsilon_F^2}\right], \quad (3.47)$$

$$P = \frac{2}{5} n \left[\left(\frac{1}{3n\pi^2}\right) \left(\frac{2m}{h}\right)^{\frac{3}{2}} \epsilon_F^{\frac{5}{2}}\right] \left[1 + \frac{5\pi^2}{12\beta^2 \epsilon_F^2}\right], \quad (3.48)$$

$$P = \frac{2}{5} n \epsilon_F \left[1 + \frac{5\pi^2}{12\beta^2 \epsilon_F^2}\right], \quad (3.49)$$

$$P = \frac{2}{5} n K_B T_F \left[1 + \frac{5\pi^2}{12} \left(\frac{K_B T}{K_B T_F}\right)^2\right], \quad (3.50)$$

$$P = \frac{2}{5} n K_B T_F \left[1 + \frac{5\pi^2}{12} \left(\frac{T}{T_F}\right)^2\right]. \quad (3.51)$$

This is perturbed Fermi pressure in 1D at non zero temperature ($T > 0$ and $T < T_F$). Compare equation (3.29) to equation (3.51) to get perturbed Fermi velocity given as:

$$v_F^2 = \frac{6}{5} \frac{K_B T_F}{m} \left[1 + \frac{5\pi^2}{12} \left(\frac{T}{T_F}\right)^2\right].$$

3.2 Modeling of the Problem

For the theoretical analysis of the problem consider a spatially uniform, homogeneous, low temperature, high density, semiconductor plasma in an external magnetic field in z-direction $B_0 \hat{z}$. Electron beams are an energy source to excite the species of semiconductor plasma. The excitation of electron and hole results in electrostatic modes in semiconductor plasma. The stability/instability of these modes can play an important role in the application of semiconductor plasma. If we want to check whether our plasma is in stable condition or unstable condition, we must check whether any net forces can accelerate the charged particles in the plasma. Other-

wise, the plasma is in equilibrium. Then to check plasma stability we must check the growth, oscillation, and damping of the perturbation. The growth rate of the wave tells us the instability of the plasma system. The electron beam is moving with velocity $v_0 \parallel B_0$ with equilibrium number density n_{b0} .

In semiconductor plasma, we have three separate fluids electrons, holes, and beam-electrons. For this multi-fluid system, we have a system of equations in the QHD model in 3D.

$$m_j^* n_j \left(\frac{\partial v_j}{\partial t} + v_j \cdot \nabla v_j \right) = n_j q_j \left(E + \frac{1}{c} v_j \times B_0 \right) - \nabla P_j + \frac{\hbar^2}{4m_j^*} \nabla (\nabla^2 n_j) - \nabla n_j V_{j,xc}. \quad (3.52)$$

$$\frac{\partial n_j}{\partial t} + \nabla \cdot (v_j n_j) = 0. \quad (3.53)$$

In above multi-fluid equations j stands for for semiconductor species electrons(e), holes(h) and beam electrons (b). m^* is the effective mass of j th species. E and B_0 are the electric field and unperturbed magnetic field. v_j , n_j , $V_{j,xc}$, q_j , P_j , are velocity, number density, the exchange and correlation potential, charge magnitude, and perturbed Fermi pressure of j th species, respectively.

3.2.1 Perturbed Velocity

$$\left(\frac{\partial v_j}{\partial t} + v_j \cdot \nabla v_j \right) = \frac{q_j}{m_j^*} \left(E + \frac{1}{c} v_j \times B_0 \right) - \frac{\nabla P_j}{n_j m_j^*} + \frac{\hbar^2}{4m_j^{*2} n_j} \nabla (\nabla^2 n_j) - \frac{\nabla n_j V_{j,xc}}{n_j m_j^*}. \quad (3.54)$$

Introducing perturbation of the type,

$$v_j \rightarrow v_{j0} + v_{j1}$$

$$n_j \rightarrow n_{j0} + n_{j1}$$

All of these perturbed quantities are equal to the sinusoidal form $e^{i(-\omega t + k_x \hat{x} + k_z \hat{z})}$ where ω is angular frequency and k is wave vector. So we can write,

$$v_{j1} = v_{j1} e^{i(-\omega t + k_x \hat{x} + k_z \hat{z})}$$

$$n_{j1} = n_{j1} e^{i(-\omega t + k_x \hat{x} + k_z \hat{z})}$$

linearize equation (3.54) to get,

$$\left(\frac{\partial v_{j1}}{\partial t} + v_{j0} \cdot \nabla v_{j1} \right) = \frac{q_j}{m_j^*} \left(E + \frac{1}{c} v_{j1} \times B_0 \right) - \frac{\nabla P_j}{n_{j0} m_j^*} + \frac{h^2}{4m_j^{*2} n_{j0}} \nabla (\nabla^2 n_{j1}) - \frac{\nabla n_{j1} V_{j,xc}}{n_{j0} m_j^*}, \quad (3.55)$$

As in the case of electrostatic waves, the time-varying magnetic field is zero i.e; $\frac{\partial B}{\partial t} = 0$. So Maxwell equation will become $(\nabla \times E)_L = 0$, which means that the electric field associated with the electrostatic model is curl-free, and it can be represented as the gradient of a scalar potential given as:

$$E = -\nabla \phi.$$

$$\left(\frac{\partial v_{j1}}{\partial t} + v_{j0} \cdot \nabla v_{j1} \right) = \frac{q_j}{m_j^*} \left(-\nabla \phi + \frac{1}{c} v_{j1} \times B_0 \right) - \frac{\nabla P_j}{n_{j0} m_j^*} + \frac{h^2}{4m_j^{*2} n_{j0}} \nabla (\nabla^2 n_{j1}) - \frac{\nabla n_{j1} V_{j,xc}}{n_{j0} m_j^*}, \quad (3.56)$$

Lorentz force

1st term on R.H.S is the Lorentz force in Gaussian (cgs) units in the presence of both electric and unperturbed magnetic field. For $v_j = v_{jx}\hat{x} + v_{jy}\hat{y} + v_{jz}\hat{z}$ and $B = B_0\hat{z}$ we get,

$$v_j \times B_0 = v_{jy}B_0\hat{x} - v_{jx}B_0\hat{y},$$

$$\frac{q_j}{m_j^*}(E + \frac{1}{c}v_j \times B_0) = \frac{q_j}{m_j^*}[-\nabla\phi + \frac{1}{c}(v_{jy}B_0\hat{x} - v_{jx}B_0\hat{y})].$$

Perturbed Fermi Pressure

2nd term on R.H.S is the gradient of perturbed Fermi pressure. The thermodynamic equation of state is given as:

$$P = P_0\left(\frac{n}{n_0}\right)^\gamma,$$

where exponent is given as $\gamma = 3$ for 1D, $P_0 = \frac{2}{3}n_0E_F$, is the Fermi pressure at $T = 0K$, $E_F = \frac{1}{2}mv_F^2$, is the Fermi energy in 1D and v_F is the Fermi velocity. The corresponding Fermi pressure will become,

$$P = \frac{mv_F^2}{3n_0^2}n^3.$$

we can use the above equation even for 3D although $\gamma = \frac{D+2}{D}$ which give $\frac{5}{3}$ in 3D. This can affect our results because we are dealing with linear wave propagation that is a 1D phenomenon, and no energy is exchanged in the other two directions.

so,

$$\nabla P_j = m_j^*v_{Fj}^2\nabla n_{j1}.$$

where $v_{Fj}^2 = \frac{6}{5}\frac{K_B T_{Fj}}{m_j^*}[1 + \frac{5}{12}\pi^2(\frac{T}{T_{Fj}})^2]$, is the Fermi velocity at non zero temperature.

$$\frac{\nabla P_j}{n_{j0}m_j^*} = \frac{1}{n_{j0}m_j^*}m_j^*v_{Fj}^2\nabla n_{j1} = v_{Fj}^2\nabla\frac{n_{j1}}{n_{j0}}.$$

Bohm Potential

3rd term on R.H.S is the Bohm potential given as, $\frac{\hbar^2}{4m_j^{*2}n_{j0}}\nabla(\nabla^2n_{j1})$.

Exchange-Correlation Potential

4th term on R.H.S is the exchange-correlation potential. This phenomenon appears because of anti-symmetric particles. The electron exchange and correlation effects incorporate a short electric potential that depends only on the number density of the charge carriers. It is given as:

$$V_{j,xc} = \frac{0.985}{3} \left(\frac{q_j^2}{\epsilon}\right) n_{j0}^{\frac{1}{3}} + \frac{0.986 \times 0.034}{3a_{bj}^*} \left(\frac{q_j^2}{\epsilon}\right) \frac{18.37a_{Bj}^* n_{j0}^{\frac{1}{3}}}{1 + 18.37a_{Bj}^* n_{j0}^{\frac{1}{3}}}.$$

where $a_{Bj}^* = \frac{\epsilon\hbar^2}{m_j q_j^2}$ is the Bohr radius, ϵ is the dielectric constant and q_j is the charge magnitude. We get,

$$\left(\frac{\partial v_{j1}}{\partial t} + v_{j0} \cdot \nabla v_{j1}\right) = \frac{q_j}{m_j^*} \left[-\nabla\phi + \frac{1}{c}(v_{jy}B_0\hat{x} - v_{jx}B_0\hat{y})\right] - v_F^2 \nabla \frac{n_{j1}}{n_{j0}} + \frac{\hbar^2}{4m_j^{*2}n_{j0}} \nabla(\nabla^2n_{j1}) - \frac{\nabla n_{j1} V_{j,xc}}{n_{j0}m_j^*}, \quad (3.57)$$

now Fourier transform above equation w.r.t space and time, by introducing $\frac{\partial}{\partial t} \rightarrow -i\omega$, $\nabla \rightarrow ik$. This will transform the differential equation into a simple algebraic equation given as:

$$-i[w - k \cdot v_0]v_{j1} = \frac{-ikq_j\phi}{m_j^*} - \frac{q_j B_0}{m_j^* c} v_{jx}\hat{y} + \frac{q_j B_0}{m_j^* c} v_{jy}\hat{x} - ikv_F^2 \left(\frac{n_{j1}}{n_{j0}}\right) - \frac{i\hbar^2 k^3}{4m_j^{*2}} \left(\frac{n_{j1}}{n_{j0}}\right) - \frac{ikV_{j,xc}}{m_j^*} \left(\frac{n_{j1}}{n_{j0}}\right), \quad (3.58)$$

where $w - k \cdot v_0 \rightarrow \omega^*$ is the Doppler shift in frequency and $\omega_{cj} \rightarrow \frac{q_j B_0}{m_j^* c}$ is the cyclotron

or gyro frequency of j th species. we get,

$$-i\omega^*v_{j1} = \frac{-ikq_j\phi}{m_j^*} - \omega_{cj}v_{jx}\hat{y} + \omega_{cj}v_{jy}\hat{x} - ikv_F^2\left(\frac{n_{j1}}{n_{j0}}\right) - \frac{ih^2k^3}{4m_j^{*2}}\left(\frac{n_{j1}}{n_{j0}}\right) - \frac{ikV_{j,xc}}{m_j^*}\left(\frac{n_{j1}}{n_{j0}}\right), \quad (3.59)$$

$$\omega^*v_{j1} = \frac{kq_j\phi}{m_j^*} + \frac{\omega_{cj}}{i}v_{jx}\hat{y} - \frac{\omega_{cj}}{i}v_{jy}\hat{x} + kv_F^2\left(\frac{n_{j1}}{n_{j0}}\right) + \frac{h^2k^3}{4m_j^{*2}}\left(\frac{n_{j1}}{n_{j0}}\right) + \frac{kV_{j,xc}}{m_j^*}\left(\frac{n_{j1}}{n_{j0}}\right), \quad (3.60)$$

$$\omega^*v_{j1} = \frac{kq_j\phi}{m_j^*} + \frac{\omega_{cj}}{i}v_{jx}\hat{y} - \frac{\omega_{cj}}{i}v_{jy}\hat{x} + \left(\frac{n_{j1}}{n_{j0}}\right)\left[v_F^2 + \frac{h^2k^2}{4m_j^{*2}} + \frac{V_{j,xc}}{m_j^*}\right]k, \quad (3.61)$$

$$\omega^*v_{j1} = \frac{kq_j\phi}{m_j^*} + \frac{\omega_{cj}}{i}v_{jx}\hat{y} - \frac{\omega_{cj}}{i}v_{jy}\hat{x} + \left(\frac{n_{j1}}{n_{j0}}\right)\left[v_{Fj}^2\left(1 + \frac{h^2k^2}{4m_j^{*2}v_{Fj}^2}\right) + \frac{V_{j,xc}}{m_j^*}\right]k, \quad (3.62)$$

where,

$$\frac{h^2k^2}{4m_j^{*2}v_{Fj}^2} = \gamma_j,$$

$$v_{Fj}^2\left(1 + \frac{h^2k^2}{4m_j^{*2}v_{Fj}^2}\right) = v_{Fj}^2(1 + \gamma_j),$$

$$v_{Fj}^2(1 + \gamma_j) = v_{Fj}'^2,$$

and,

$$v_{Fj}\sqrt{(1 + \gamma_j)} = v_{Fj}'^2.$$

This speed contain the effects of both the Bohm potential (quantum effects) and the perturbed Fermi pressure. The exchange-correlation speed of j th species is given as:

$$V_{j,xc} = m_j^* v_{j,xc}^2 \rightarrow \frac{V_{j,xc}}{m_j^*} = v_{j,xc}^2.$$

we get,

$$\omega^* v_{j1} = \frac{kq_j\phi}{m_j^*} + \frac{\omega_{cj}}{i} v_{jx}\hat{y} - \frac{\omega_{cj}}{i} v_{jy}\hat{x} + \left(\frac{n_{j1}}{n_{j0}}\right)[v_{Fj}^2 + v_{j,xc}^2]k \quad (3.63)$$

$$v_{Fj}^2 + v_{j,xc}^2 = v_{Fj}^{\prime 2}$$

$$\omega^* v_{j1} = \frac{kq_j\phi}{m_j^*} + \frac{\omega_{cj}}{i} v_{jx}\hat{y} - \frac{\omega_{cj}}{i} v_{jy}\hat{x} + \left(\frac{n_{j1}}{n_{j0}}\right)v_{Fj}^{\prime 2}k, \quad (3.64)$$

$$\omega^* v_{j1} = \frac{kq_j\phi}{m_j^*} - i\omega_{cj}v_{jx}\hat{y} + i\omega_{cj}v_{jy}\hat{x} + \left(\frac{n_{j1}}{n_{j0}}\right)v_{Fj}^{\prime 2}k. \quad (3.65)$$

The components of above equation are given as:

x-component

$$\omega^* v_{j1x} = \frac{q_j\phi}{m_j^*}k_x + i\omega_{cj}v_{jy} + \left(\frac{n_{j1}}{n_{j0}}\right)v_{Fj}^{\prime 2}k_x, \quad (3.66)$$

$$\omega^* v_{j1x} - i\omega_{cj}v_{jy} = \frac{q_j\phi}{m_j^*}k_x + \left(\frac{n_{j1}}{n_{j0}}\right)v_{Fj}^{\prime 2}k_x, \quad (3.67)$$

$$\omega^* [v_{j1x} - \frac{i\omega_{cj}v_{jy}}{\omega^*}] = \frac{q_j\phi}{m_j^*}k_x + \left(\frac{n_{j1}}{n_{j0}}\right)v_{Fj}^{\prime 2}k_x, \quad (3.68)$$

$$\omega^* [v_{j1x} - \frac{i\omega_{cj}v_{jy}}{\omega^*}] = \frac{q_j}{m_j^*}[\phi + \frac{m_j^*}{q_j}\left(\frac{n_{j1}}{n_{j0}}\right)v_{Fj}^{\prime 2}]k_x, \quad (3.69)$$

$$\Phi = [\phi + \frac{m_j^*}{q_j} (\frac{n_{j1}}{n_{j0}}) v_{Fj}^2].$$

This is the effective potential which includes the electrostatic potential " ϕ ".

$$\omega^* [v_{j1x} - \frac{i\omega_{cj} v_{jy}}{\omega^*}] = \frac{q_j \Phi}{m_j^*} k_x. \quad (3.70)$$

y-component

$$\omega^* v_{j1y} = -i\omega_{cj} v_{jx}, \quad (3.71)$$

$$v_{j1y} = -\frac{i\omega_{cj}}{\omega^*} v_{jx}. \quad (3.72)$$

put y-component in x-component to get,

$$\omega^* v_{j1x} - \frac{i\omega_{cj}}{\omega^*} (-\frac{i\omega_{cj}}{\omega^*} v_{jx}) = \frac{q_j \Phi}{m_j^*} k_x, \quad (3.73)$$

$$\omega^* [v_{jx} - \frac{\omega_{cj}^2}{\omega^{*2}} v_{jx}] = \frac{q_j \Phi}{m_j^*} k_x, \quad (3.74)$$

$$v_{jx} [1 - \frac{\omega_{cj}^2}{\omega^{*2}}] = \frac{q_j \Phi}{m_j^* \omega^*} k_x, \quad (3.75)$$

$$v_{jx} = \frac{q_j \Phi}{m_j^* \omega^*} [\frac{\omega^{*2} - \omega_{cj}^2}{\omega^{*2}}]^{-1} k_x, \quad (3.76)$$

$$v_{jx} = \frac{q_j \Phi}{m_j^* \omega^*} [\frac{\omega^{*2}}{\omega^{*2} - \omega_{cj}^2}] k_x. \quad (3.77)$$

now put x-component in y-component to get,

$$v_{jy} = -\frac{i\omega_{cj}}{\omega^*} [\frac{q_j \Phi}{m_j^* \omega^*} (\frac{\omega^{*2}}{\omega^{*2} - \omega_{cj}^2})] k_x, \quad (3.78)$$

$$v_{jy} = -\frac{q_j \Phi}{m_j^* \omega^*} \left(\frac{i\omega^* \omega_{cj}}{\omega^{*2} - \omega_{cj}^2} \right) k_x. \quad (3.79)$$

z-component

$$\omega^* v_{j1z} = \frac{q_j \phi}{m_j^*} k_z + \left(\frac{n_{j1}}{n_{j0}} \right) v_{Fj}'' k_z, \quad (3.80)$$

$$v_{j1z} = \frac{q_j}{m_j^* \omega^*} \left[\phi + \frac{m_j^*}{q_j} \left(\frac{n_{j1}}{n_{j0}} \right) v_{Fj}'' \right] k_z, \quad (3.81)$$

$$v_{j1z} = \frac{q_j \Phi}{m_j^* \omega^*} k_z, \quad (3.82)$$

the perturbed velocity of j th species can be obtained by,

$$v_j = v_{jx} \hat{x} + v_{jy} \hat{y} + v_{jz} \hat{z}.$$

$$v_j = \frac{q_j \Phi}{m_j^* \omega^*} \left(\frac{\omega^{*2}}{\omega^{*2} - \omega_{cj}^2} \right) k_x \hat{x} - \frac{q_j \Phi}{m_j^* \omega^*} \left(\frac{i\omega^* \omega_{cj}}{\omega^{*2} - \omega_{cj}^2} \right) k_x \hat{y} + \frac{q_j \Phi}{m_j^* \omega^*} k_z \hat{z}, \quad (3.83)$$

$$v_j = \frac{q_j \Phi}{m_j^* \omega^*} \left[\frac{\omega^{*2}}{\omega^{*2} - \omega_{cj}^2} k_x \hat{x} - \frac{i\omega^* \omega_{cj}}{\omega^{*2} - \omega_{cj}^2} k_x \hat{y} + k_z \hat{z} \right]. \quad (3.84)$$

3.2.2 Perturbed Number Density

Perturbed number density of j th species can be obtained by using equation of continuity given as:

$$\frac{\partial n_j}{\partial t} + \nabla \cdot (v_j n_j) = 0.$$

now introduce perturbation of the form,

$$n_j \rightarrow n_{j0} + n_{j1}$$

$$v_j \rightarrow v_{j0} + v_{j1}$$

we get,

$$\frac{\partial}{\partial t}[n_{j0} + n_{j1}] + \nabla \cdot [n_{j0} + n_{j1}][v_{j0} + v_{j1}] = 0, \quad (3.85)$$

$$\frac{\partial n_{j0}}{\partial t} + \frac{\partial n_{j1}}{\partial t} + \nabla \cdot [n_{j0}v_{j0} + n_{j0}v_{j1} + n_{j1}v_{j0} + n_{j1}v_{j1}] = 0, \quad (3.86)$$

neglect the non linear terms such as:

$$\frac{\partial n_{j0}}{\partial t} = 0, \nabla v_{j0} = 0, \nabla n_{j0} = 0$$

we get,

$$\frac{\partial n_{j1}}{\partial t} + n_{j0} \nabla \cdot v_{j1} + v_{j0} \nabla \cdot v_{j1} = 0 \quad (3.87)$$

$$\frac{\partial n_{j1}}{\partial t} + v_{j0} \nabla \cdot v_{j1} = -n_{j0} \nabla \cdot v_{j1}, \quad (3.88)$$

$$n_{j1}[-i\omega + v_{j0} \cdot ik] = -n_{j0} ik \cdot v_{j1}, \quad (3.89)$$

$$n_{j1}[\omega - k \cdot v_{j0}] = n_{j0} k \cdot v_{j1}, \quad (3.90)$$

$$n_{j1} \omega^* = n_{j0} k \cdot v_{j1}, \quad (3.91)$$

$$n_{j1} = \frac{n_{j0}k.v_{j1}}{\omega^*}, \quad (3.92)$$

now put value of v_{j1} to get,

$$n_{j1} = \frac{n_{j0}}{\omega^*} (k_x \hat{x} + k_z \hat{z}) \cdot \frac{q_j \Phi}{m_j^* \omega^*} \left[\frac{\omega^{*2}}{\omega^{*2} - \omega_{cj}^2} k_x \hat{x} - \frac{i\omega^* \omega_{cj}}{\omega^{*2} - \omega_{cj}^2} k_x \hat{y} + k_z \hat{z} \right], \quad (3.93)$$

$$n_{j1} = \frac{n_{j0}}{\omega^*} \frac{q_j \Phi}{m_j^* \omega^*} \left[\frac{\omega^{*2}}{\omega^{*2} - \omega_{cj}^2} k_x^2 + k_z^2 \right], \quad (3.94)$$

$$n_{j1} = \frac{n_{j0} q_j}{m_j^* \omega^{*2}} \left[\frac{\omega^{*2}}{\omega^{*2} - \omega_{cj}^2} k_x^2 + k_z^2 \right] \Phi, \quad (3.95)$$

$$n_{j1} = \frac{n_{j0} q_j}{m_j^* \omega^{*2}} \left[\frac{\omega^{*2}}{\omega^{*2} - \omega_{cj}^2} k_x^2 + k_z^2 \right] \left[\phi + \frac{m_j^*}{q_j} \left(\frac{n_{j1}}{n_{j0}} \right) v_{j,xc}'' \right], \quad (3.96)$$

$$n_{j1} = \frac{n_{j0} q_j}{m_j^* \omega^{*2}} \left[\frac{\omega^{*2}}{\omega^{*2} - \omega_{cj}^2} k_x^2 + k_z^2 \right] \phi + \frac{n_{j0} q_j}{m_j^* \omega^{*2}} \left[\frac{\omega^{*2}}{\omega^{*2} - \omega_{cj}^2} k_x^2 + k_z^2 \right] \left[\frac{m_j^*}{q_j} \left(\frac{n_{j1}}{n_{j0}} \right) v_{Fj}'' \right], \quad (3.97)$$

$$n_{j1} = \frac{n_{j0} q_j}{m_j^* \omega^{*2}} \left[\frac{\omega^{*2}}{\omega^{*2} - \omega_{cj}^2} k_x^2 + k_z^2 \right] \phi + \frac{n_{j1}}{\omega^{*2}} v_{Fj}'' \left[\frac{\omega^{*2}}{\omega^{*2} - \omega_{cj}^2} k_x^2 + k_z^2 \right], \quad (3.98)$$

$$n_{j1} \left[1 - \frac{v_{Fj}''}{\omega^{*2}} \left[\frac{\omega^{*2}}{\omega^{*2} - \omega_{cj}^2} k_x^2 + k_z^2 \right] \right] = \frac{n_{j0} q_j}{m_j^* \omega^{*2}} \left[\frac{\omega^{*2}}{\omega^{*2} - \omega_{cj}^2} k_x^2 + k_z^2 \right] \phi, \quad (3.99)$$

$$n_{j1} = \frac{\frac{n_{j0} q_j}{m_j^*} \left[\frac{k_x^2}{\omega^{*2} - \omega_{cj}^2} + \frac{k_z^2}{\omega^{*2}} \right] \phi}{\left[1 - \frac{v_{Fj}'' k_x^2}{\omega^{*2} - \omega_{cj}^2} - \frac{v_{Fj}'' k_z^2}{\omega^{*2}} \right]}. \quad (3.100)$$

3.2.3 Dielectric Response Function

We are interested in the response of the system to some external electron beam moving with velocity v_0 (in other words external charges and currents). The system show response to these external charges and currents and generates internal charges and currents, and their corresponding internal electric and magnetic fields E_{int} and B_{int} . Instead of taking these internal and external charges and currents separately, we can consider that these external charges and currents are the part of the system and produced in the localized apace within the system. Theoretically, to do that we consider a single Fourier component of a wave-packet out of all wave-packets. Of course, this is experimentally difficult to analyze, because experimentally they are outside the system. One way to deal with this situation in the electrostatic case is to introduce the polarization field P because polarization vanishes outside the system just like D which means they had a transverse component outside the system. Polarization can be written in the form of charge density given as:

$$\begin{aligned}\nabla \cdot P &= -\rho, \\ \frac{\nabla \cdot \chi_j E}{4\pi} &= -q_j n_{j1}, \\ -\frac{\chi_j \nabla^2 \phi}{4\pi} &= -q_j n_{j1}, \\ \frac{\chi_j k^2 \phi}{4\pi} &= -q_j n_{j1}, \\ n_{j1} &= -\frac{k^2 \chi_j \phi}{4\pi q_j}.\end{aligned}$$

This expression relates the number density with the dielectric susceptibility. Now, after putting the value of perturbed number density the dielectric susceptibility for j th species is given as:

$$\chi_j = -\frac{4\pi q_j}{k^2 \phi} n_{j1}. \quad (3.101)$$

$$\chi_j = -\frac{4\pi q_j^2 n_{j0}}{k^2 m_j^*} \frac{\left[\frac{k_x^2}{\omega^{*2} - \omega_{cj}^2} + \frac{k_z^2}{\omega^{*2}} \right]}{\left[1 - \frac{v_{Fj}''^2 k_x^2}{\omega^{*2} - \omega_{cj}^2} - \frac{v_{Fj}''^2 k_z^2}{\omega^{*2}} \right]}, \quad (3.102)$$

where $\omega_{pj}^2 = \frac{4\pi n_{j0} q_j^2}{m_j^*}$, is plasma beam frequency of j th species.

$$\chi_j = -\frac{\omega_{pj}^2 \left[\frac{k_x^2}{\omega^{*2} - \omega_{cj}^2} + \frac{k_z^2}{\omega^{*2}} \right]}{k^2 \left[1 - \frac{v_{Fj}''^2 k_x^2}{\omega^{*2} - \omega_{cj}^2} - \frac{v_{Fj}''^2 k_z^2}{\omega^{*2}} \right]}. \quad (3.103)$$

the dielectric constant for electrostatic waves is given as:

$$\epsilon(\omega, k) = 1 + \sum_j \chi_j = 0,$$

or,

$$1 + \chi_b + \chi_e + \chi_h = 0. \quad (3.104)$$

by reducing the expression of (3.103) according to the conditions for electrons, beam and holes we get,

Dielectric Susceptibility of Electron Beam

As $k_x \gg k_z$ so, we can neglect k_z .

$$\chi_b \approx -\frac{\omega_{pb}^2 \left[\frac{k_x^2}{(\omega - k \cdot v_0)^2} \right]}{k^2 \left[1 - \frac{v_{Fb}''^2 k_x^2}{(\omega - k \cdot v_0)^2} \right]}. \quad (3.105)$$

The effective speed that includes thermal, exchange-correlation and the Bohm effects is given as:

$$v_{Fj}''2 = [v_{j,xc}^2 + v_{Fj}^2(1 + \frac{h^2 k^2}{4m_j^* v_{Fj}^2})].$$

For electron beam the effective speed have no exchange correlation and quantum effect contribution. we are left with only thermal speed of beam electrons at equilibrium given as:

$$v_{Fb}''2 = v_{Fb}^2 = \frac{k_B h^2 (3\pi^2 n_{b0})^{2/3}}{m_e^2}.$$

the Fermi temperature of beam electrons is given as:

$$T_{Fb} = T_b = \frac{h^2 (3\pi^2 n_{b0})^{2/3}}{2m_e}.$$

the effective speed will become,

$$v_{Fb}''2 = v_{Fb}^2 = \frac{2k_B T_b}{m_e} = v_b^2.$$

$$\chi_b \approx -\frac{\omega_{pb}^2 [\frac{k_x^2}{(\omega - k \cdot v_0)^2}]}{k^2 [1 - \frac{v_b^2 k_x^2}{(\omega - k \cdot v_0)^2}]} \quad (3.106)$$

The phase speed ω/k of LHW is smaller than the speed of the electron beam v_0 i.e.

$k \cdot v_0 \gg \omega$, $\frac{\omega}{k} \ll v_0$ we get,

$$\chi_b \approx -\frac{\omega_{pb}^2}{(v_0^2 - v_b^2)k^2}. \quad (3.107)$$

This is the dielectric susceptibility of electron beam with $\omega_{pb}^2 = \frac{4\pi n_{b0} q_b^2}{m_e}$, is the oscillation frequency of beam electrons.

Dielectric Susceptibility of Electrons

As $k_x \gg k_z$ so, we can neglect k_z to get,

$$\chi_e \approx -\frac{\omega_{pe}^2 \left[\frac{k_x^2}{(\omega - k \cdot v_0)^2 - \omega_{ce}^2} \right]}{k^2 \left[1 - \frac{v_{Fe}''^2 k_x^2}{(\omega - k \cdot v_0)^2 - \omega_{ce}^2} \right]}, \quad (3.108)$$

$$\chi_e \approx -\frac{\omega_{pe}^2 \left[\frac{k_x^2}{\omega^2 - \omega_{ce}^2} \right]}{k^2 \left[1 - \frac{v_{Fe}''^2 k_x^2}{\omega^2 - \omega_{ce}^2} \right]}, \quad (3.109)$$

$$\because \omega \ll \omega_{ce}, \omega_{pe}$$

where $\omega - k \cdot v_0 \approx 0$ for the Cerenkov interaction (the resonance condition) [45][46].

$$\chi_e \approx -\frac{\omega_{pe}^2 \left[\frac{k_x^2}{-\omega_{ce}^2} \right]}{k^2 \left[1 - \frac{v_{Fe}''^2 k_x^2}{-\omega_{ce}^2} \right]}, \quad (3.110)$$

$$\chi_e \approx \frac{\omega_{pe}^2}{(\omega_{ce}^2 + v_{Fe}''^2 k_x^2)} \frac{k_x^2}{k^2}. \quad (3.111)$$

This is the dielectric susceptibility of electrons with $\omega_{pe}^2 = \frac{4\pi n_e q_e^2}{m_e^*}$, is the oscillation frequency of electrons. $\omega_{ce} = \frac{eB_0}{m_e^* c}$, is the cyclotron frequency of electrons.

$v_{Fe}''^2 = [v_{e,xc}^2 + v_{Fe}^2 (1 + \frac{\hbar^2 k^2}{4m_e^* v_{Fe}^2})]$, is the effective speed that include thermal, exchange-correlation, and Bohm effects.

Dielectric Susceptibility of Holes

As $k_x \gg k_z$ so, we can neglect k_z ,

$$\chi_h \approx -\frac{\omega_{ph}^2 \left[\frac{k_x^2}{(\omega - k \cdot v_0)^2 - \omega_{ch}^2} \right]}{k^2 \left[1 - \frac{v_{Fh}''^2 k_x^2}{(\omega - k \cdot v_0)^2 - \omega_{ch}^2} \right]}, \quad (3.112)$$

$$\omega \gg \omega_{ch}, \omega_{ph}$$

$$\chi_h \approx -\frac{\omega_{ph}^2 \left[\frac{k_x^2}{\omega^2 - \omega_{ch}^2} \right]}{k^2 \left[1 - \frac{v_{Fh}''^2 k_x^2}{\omega^2 - \omega_{ch}^2} \right]}, \quad (3.113)$$

$$\chi_h \approx -\frac{\omega_{ph}^2}{(\omega^2 - \omega_{ch}^2 - v_{Fh}''^2 k_x^2)} \frac{k_x^2}{k^2}. \quad (3.114)$$

This is the dielectric susceptibility of holes with $\omega_{ph}^2 = \frac{4\pi n_h q_h^2}{m_h^*}$, is the oscillation frequency of holes, $\omega_{ch} = \frac{eB_0}{m_h^* c}$ is the cyclotron frequency and $v_{Fh}''^2 = [v_{h,xc}^2 + v_{Fh}^2 (1 + \frac{h^2 k^2}{4m_h^{*2} v_{Fh}^2})]$ is the effective speed.

3.2.4 Dispersion Relation

As,

$$1 + \chi_b + \chi_e = -\chi_h \quad (3.115)$$

$$\frac{\omega_{ph}^2}{(\omega^2 - \omega_{ch}^2 - v_{Fh}''^2 k_x^2)} \frac{k_x^2}{k^2} = 1 - \frac{\omega_{pb}^2}{(v_0^2 - v_b^2)k^2} + \frac{\omega_{pe}^2}{(\omega_{ce}^2 + v_{Fe}''^2 k_x^2)} \frac{k_x^2}{k^2}, \quad (3.116)$$

$$\frac{\omega_{ph}^2}{(\omega^2 - \omega_{ch}^2 - v_{Fh}''^2 k_x^2)} \frac{k_x^2}{k^2} = \frac{k^2(v_0^2 - v_b^2)(\omega_{ce}^2 + v_{Fe}''^2 k_x^2) - \omega_{pb}^2(\omega_{ce}^2 + v_{Fe}''^2 k_x^2) + \omega_{pe}^2 k_x^2(v_0^2 - v_b^2)}{k^2(v_0^2 - v_b^2)(\omega_{ce}^2 + v_{Fe}''^2 k_x^2)}, \quad (3.117)$$

$$(\omega^2 - \omega_{ch}^2 - v_{Fh}''^2 k_x^2) = \frac{\omega_{ph}^2 k_x^2 (v_0^2 - v_b^2) (\omega_{ce}^2 + v_{Fe}''^2 k_x^2)}{k^2 (v_0^2 - v_b^2) (\omega_{ce}^2 + v_{Fe}''^2 k_x^2) - \omega_{pb}^2 (\omega_{ce}^2 + v_{Fe}''^2 k_x^2) + \omega_{pe}^2 k_x^2 (v_0^2 - v_b^2)}, \quad (3.118)$$

$$\omega^2 = \omega_{ch}^2 + v_{Fh}''^2 k_x^2 + \frac{\omega_{ph}^2 k_x^2 (v_0^2 - v_b^2) (\omega_{ce}^2 + v_{Fe}''^2 k_x^2)}{k^2 (v_0^2 - v_b^2) (\omega_{ce}^2 + v_{Fe}''^2 k_x^2) + \omega_{pe}^2 k_x^2 (v_0^2 - v_b^2) - \omega_{pb}^2 (\omega_{ce}^2 + v_{Fe}''^2 k_x^2)}, \quad (3.119)$$

$$\omega^2 = \omega_{ch}^2 + v_{Fh}''^2 k_x^2 + \frac{\omega_{ph}^2 k_x^2 (v_0^2 - v_b^2) (\omega_{ce}^2 + v_{Fe}''^2 k_x^2)}{[k^2 (\omega_{ce}^2 + v_{Fe}''^2 k_x^2) + \omega_{pe}^2 k_x^2] (v_0^2 - v_b^2) - \omega_{pb}^2 (\omega_{ce}^2 + v_{Fe}''^2 k_x^2)}, \quad (3.120)$$

$$\omega^2 = \omega_{lh}^2 \delta + v_{Fh}''^2 k_x^2 + \frac{\omega_{ph}^2 k_x^2 (v_0^2 - v_b^2) (\omega_{ce}^2 + v_{Fe}''^2 k_x^2)}{[k^2 (\omega_{ce}^2 + v_{Fe}''^2 k_x^2) + \omega_{pe}^2 k_x^2] (v_0^2 - v_b^2) - \omega_{pb}^2 (\omega_{ce}^2 + v_{Fe}''^2 k_x^2)}. \quad (3.121)$$

where, $\omega_{lh}^2 = \omega_{ch} \omega_{ch}$ and $\delta = \frac{m_e^*}{m_h^*}$. This is the linear dispersion relation for L.H.Ws in an electron-hole plasma that is pumped by an electron beam, it includes the exchange correlation effects, the quantum effects and the thermal degenerate effects.

3.2.5 Analytical Study L.H.Ws in Quantum Semiconductor Plasma

Normalize equation (3.120) with scale ω_{ph}^2 to study LHWs in quantum semiconductor plasma induced by electron beam.

$$\frac{\omega^2}{\omega_{ph}^2} = \frac{\omega_{ch}^2}{\omega_{ph}^2} + \frac{v_{Fh}''^2 k_x^2}{\omega_{ph}^2} + \frac{k_x^2 (v_0^2 - v_b^2) (\omega_{ce}^2 + v_{Fe}''^2 k_x^2)}{[k^2 (\omega_{ce}^2 + v_{Fe}''^2 k_x^2) + \omega_{pe}^2 k_x^2] (v_0^2 - v_b^2) - \omega_{pb}^2 (\omega_{ce}^2 + v_{Fe}''^2 k_x^2)}, \quad (3.122)$$

$$\tilde{\omega}^2 = \tilde{\omega}_{ch}^2 + \tilde{v}_{Fh}''^2 \tilde{k}_x^2 + \frac{\omega_{ph}^2 \left(\frac{k_x^2 v_{Fh0}^2}{\omega_{ph}^2} \right) \left(\frac{v_0^2}{v_{Fh0}^2} - \frac{v_b^2}{v_{Fh0}^2} \right) (\omega_{ce}^2 + v_{Fe}''^2 k_x^2)}{[\omega_{ph}^2 \left(\frac{k_x^2 v_{Fh0}^2}{\omega_{ph}^2} \right) (\omega_{ce}^2 + v_{Fe}''^2 k_x^2) + \omega_{pe}^2 \omega_{ph}^2 \left(\frac{k_x^2 v_{Fh0}^2}{\omega_{ph}^2} \right) \left(\frac{v_0^2}{v_{Fh0}^2} - \frac{v_b^2}{v_{Fh0}^2} \right) - \omega_{pb}^2 (\omega_{ce}^2 + v_{Fe}''^2 k_x^2)]}, \quad (3.123)$$

$$\tilde{\omega}^2 = \tilde{\omega}_{ch}^2 + \tilde{v}_{Fh}''^2 \tilde{k}_x^2 + \frac{\omega_{ph}^4 \left(\frac{\omega_{ce}^2}{\omega_{ph}^2} + \frac{v_{Fe}''^2 k_x^2}{\omega_{ph}^2} \right) (\tilde{v}_0^2 - \tilde{v}_b^2) \tilde{k}_x^2}{\omega_{ph}^4 \left[\tilde{k}^2 \left(\frac{\omega_{ce}^2}{\omega_{ph}^2} + \frac{v_{Fe}''^2 k_x^2}{\omega_{ph}^2} \right) + \frac{\omega_{pe}^2}{\omega_{ph}^2} \tilde{k}_x^2 \right] (\tilde{v}_0^2 - \tilde{v}_b^2) - \omega_{ph}^4 \frac{\omega_{pb}^2}{\omega_{ph}^2} \left(\frac{\omega_{ce}^2}{\omega_{ph}^2} + \frac{v_{Fe}''^2 k_x^2}{\omega_{ph}^2} \right)}, \quad (3.124)$$

$$\tilde{\omega}^2 = \tilde{\omega}_{ch}^2 + \tilde{v}_{Fh}''^2 \tilde{k}_x^2 + \frac{(\tilde{\omega}_{ce}^2 + \tilde{v}_{Fe}''^2 \tilde{k}_x^2) (\tilde{v}_0^2 - \tilde{v}_b^2) \tilde{k}_x^2}{[\tilde{k}^2 (\tilde{\omega}_{ce}^2 + \tilde{v}_{Fe}''^2 \tilde{k}_x^2) + \tilde{\omega}_{pe}^2 \tilde{k}_x^2] (\tilde{v}_0^2 - \tilde{v}_b^2) - \tilde{\omega}_{pb}^2 (\tilde{\omega}_{ce}^2 + \tilde{v}_{Fe}''^2 \tilde{k}_x^2)}, \quad (3.125)$$

$$\tilde{\omega}^2 = \tilde{\omega}_{ch}^2 + \tilde{v}_{Fh}''^2 \tilde{k}_x^2 + \frac{(\tilde{\omega}_{ce}^2 + \tilde{v}_{Fe}''^2 \tilde{k}_x^2) (\tilde{v}_0^2 - \tilde{v}_b^2) \tilde{k}_x^2}{[\tilde{k}^2 (\tilde{\omega}_{ce}^2 + \tilde{v}_{Fe}''^2 \tilde{k}_x^2) + \tilde{\omega}_{pe}^2 \tilde{k}_x^2] (\tilde{v}_0^2 - \tilde{v}_b^2) - \tilde{\omega}_{pb}^2 (\tilde{\omega}_{ce}^2 + \tilde{v}_{Fe}''^2 \tilde{k}_x^2)}, \quad (3.126)$$

$$\tilde{\omega}^2 = \tilde{\omega}_{ch}^2 + \tilde{v}_{Fh}''^2 \tilde{k}_x^2 + \frac{\tilde{k}_x^2}{[\tilde{k}^2 + \frac{\tilde{\omega}_{pe}^2 \tilde{k}_x^2}{(\tilde{\omega}_{ce}^2 + \tilde{v}_{Fe}''^2 \tilde{k}_x^2)}] - \frac{\tilde{\omega}_{pb}^2}{(\tilde{v}_0^2 - \tilde{v}_b^2)}}. \quad (3.127)$$

where the normalized values are given as:

$$(1) \quad \tilde{\omega}^2 = \frac{\omega^2}{\omega_{ph}^2}, \quad (2) \quad \tilde{\omega}_{ch}^2 = \frac{\omega_{ch}^2}{\omega_{ph}^2}, \quad (3) \quad \tilde{\omega}_{ce}^2 = \frac{\omega_{ce}^2}{\omega_{ph}^2} = \frac{\omega_{ch}^2}{\omega_{ph}^2} \left(\frac{m_h^*}{m_e^*} \right)^2,$$

$$(4) \quad \tilde{v}_0^2 = \frac{v_0^2}{v_{Fh0}^2}, \quad (5) \quad \tilde{v}_b^2 = \frac{v_b^2}{v_{Fh0}^2} = \frac{m_h^*}{m_e} \frac{T_b}{T_{Fh0}},$$

$$(6) \quad \tilde{\omega}_{pb}^2 = \frac{\omega_{pb}^2}{\omega_{ph}^2} = \left(\frac{n_{b0}}{n_{h0}}\right) \left(\frac{m_h^*}{m_e}\right), \quad (7) \quad \tilde{\omega}_{pe}^2 = \frac{\omega_{pe}^2}{\omega_{ph}^2} = \left(\frac{n_{e0}}{n_{h0}}\right) \left(\frac{m_h^*}{m_e}\right),$$

$$(8) \quad \tilde{T}_e = \frac{T_e}{T_{Fh0}}, \quad (9) \quad \tilde{T}_h = \frac{T_h}{T_{Fh0}},$$

$$(10) \quad \tilde{v}_{e,xc}^2 = \frac{v_{e,xc}^2}{v_{Fh0}^2}, \quad (11) \quad \tilde{v}_{h,xc}^2 = \frac{v_{h,xc}^2}{v_{Fh0}^2}, \quad (12) \quad \tilde{k}^2 = \frac{v_{Fh0}^2 k^2}{\omega_{ph}^2},$$

$$(13) \quad \tilde{v}_{Fh}''^2 \tilde{k}_x^2 = \frac{v_{Fh}''^2 k_x^2}{\omega_{ph}^2} = \frac{v_{Fh}''^2}{v_{Fh0}^2} \frac{v_{Fh0}^2 k_x^2}{\omega_{ph}^2},$$

$$\tilde{v}_{Fh}''^2 \tilde{k}_x^2 = \frac{v_{Fh}''^2}{v_{Fh0}^2} \frac{v_{Fh0}^2 k^2 \cos^2 \theta}{\omega_{ph}^2},$$

$$\tilde{v}_{Fh}''^2 \tilde{k}_x^2 = \frac{v_{Fh}''^2}{v_{Fh0}^2} \tilde{k}^2 \cos^2 \theta,$$

$$\because v_{Fh}''^2 = [v_{h,xc}^2 + v_{Fh}^2 (1 + \frac{h^2 k^2}{4m_h^{*2} v_{Fh}^2})],$$

$$\tilde{v}_{Fh}''^2 \tilde{k}_x^2 = \frac{1}{v_{Fh0}^2} [v_{h,xc}^2 + v_{Fh}^2 (1 + \frac{h^2 k^2}{4m_h^{*2} v_{Fh}^2})] \tilde{k}^2 \cos^2 \theta,$$

$$\tilde{v}_{Fh}''^2 \tilde{k}_x^2 = [\frac{v_{h,xc}^2}{v_{Fh0}^2} + \frac{v_{Fh}^2}{v_{Fh0}^2} + \frac{h^2 k^2}{4m_h^{*2} v_{Fh0}^2}] \tilde{k}^2 \cos^2 \theta,$$

$$\because v_{Fh}^2 = \frac{6}{5} \frac{K_B T_h}{m_h^*} [1 + \frac{5}{12} \pi^2 (\frac{T_h}{T_{Fh0}})^2], \quad v_{Fh0}^2 = \frac{2K_B T_h}{m_h^*},$$

$$\tilde{v}_{Fh}''^2 \tilde{k}_x^2 = [\tilde{v}_{h,xc}^2 + \frac{v_{Fh0}}{v_{Fh0}} \frac{3}{5} (1 + \frac{5}{12} \pi^2 (\frac{T_h}{T_{Fh0}})^2) + \frac{h^2 \omega_{ph}^2}{4m_h^{*2} v_{Fh0}^4} \frac{k^2 v_{Fh0}^2}{\omega_{ph}^2}] \tilde{k}^2 \cos^2 \theta,$$

$$\tilde{v}_{Fh}''^2 \tilde{k}_x^2 = [\tilde{v}_{h,xc}^2 + \frac{3}{5}(1 + \frac{5}{12}\pi^2 \tilde{T}_h^2) + \frac{h^2 \omega_{ph}^2 \tilde{k}^2}{4m_h^{*2} v_{Fh0}^4}] \tilde{k}^2 \cos^2 \theta,$$

$$\tilde{v}_{Fh}''^2 \tilde{k}_x^2 = [\tilde{v}_{h,xc}^2 + \frac{3}{5}(1 + \frac{5}{12}\pi^2 \tilde{T}_h^2) + \tilde{H}^2 \tilde{k}^2] \tilde{k}^2 \cos^2 \theta,$$

$$\tilde{v}_{Fh}''^2 \tilde{k}_x^2 = [\tilde{v}_{h,xc}^2 + \frac{3}{5}(1 + \frac{5}{12}\pi^2 \tilde{T}_h^2) \{1 + \frac{\tilde{H}^2 \tilde{k}^2}{\frac{3}{5}(1 + \frac{5}{12}\pi^2 \tilde{T}_h^2)}\}] \tilde{k}^2 \cos^2 \theta.$$

$$(14) \quad \tilde{v}_{Fe}''^2 \tilde{k}_x^2 = \frac{v_{Fe}''^2 k_x^2}{\omega_{ph}^2} = \frac{v_{Fe}''^2 v_{Fh0}^2 k_x^2}{v_{Fh0}^2 \omega_{ph}^2},$$

$$\tilde{v}_{Fe}''^2 \tilde{k}_x^2 = \frac{v_{Fe}''^2 v_{Fh0}^2 k^2 \cos^2 \theta}{v_{Fh0}^2 \omega_{ph}^2},$$

$$\tilde{v}_{Fe}''^2 \tilde{k}_x^2 = \frac{v_{Fe}''^2}{v_{Fh0}^2} \tilde{k}^2 \cos^2 \theta,$$

$$\because v_{Fe}''^2 = [v_{e,xc}^2 + v_{eh}^2 (1 + \frac{h^2 k^2}{4m_h^{*2} v_{eh}^2})],$$

$$\tilde{v}_{Fe}''^2 \tilde{k}_x^2 = \frac{1}{v_{Fh0}^2} [v_{e,xc}^2 + v_{Fe}^2 (1 + \frac{h^2 k^2}{4m_e^{*2} v_{Fe}^2})] \tilde{k}^2 \cos^2 \theta,$$

$$\tilde{v}_{Fe}''^2 \tilde{k}_x^2 = [\frac{v_{e,xc}^2}{v_{Fh0}^2} + \frac{v_{Fe}^2}{v_{Fh0}^2} + \frac{h^2 k^2}{4m_e^{*2} v_{Fh0}^2}] \tilde{k}^2 \cos^2 \theta,$$

$$\because v_{Fe}^2 = \frac{6}{5} \frac{K_B T_e}{m_e^*} [1 + \frac{5}{12} \pi^2 (\frac{T_e}{T_{Fe0}})^2],$$

$$v_{Fh0}^2 = \frac{2K_B T_h}{m_h^*},$$

$$\tilde{v}_{Fe}''^2 \tilde{k}_x^2 = \left[\tilde{v}_{e,xc}^2 + \frac{T_{Fe0}}{T_{Fho}} \frac{m_h^*}{m_e^*} \frac{3}{5} \left(1 + \frac{5}{12} \pi^2 \left(\frac{T_e}{T_{Fe0}} \right)^2 \right) + \frac{h^2 \omega_{ph}^2 \frac{k^2 v_{Fho}^2}{\omega_{ph}^2}}{4m_e^{*2} v_{Fh0}^4} \right] \tilde{k}^2 \cos^2 \theta,$$

$$\therefore T_{F(e,h)0} = \frac{h^2 (3\pi^2 n_{(e,h)0})^{2/3}}{2m_{e,h}}.$$

$$\tilde{v}_{Fe}''^2 \tilde{k}_x^2 = \left[\tilde{v}_{e,xc}^2 + \left(\frac{m_h^*}{m_e^*} \right)^2 \left(\frac{n_{e0}}{n_{ho}} \right)^{2/3} \frac{3}{5} \left(1 + \frac{5}{12} \pi^2 \left(\frac{T_e}{T_{Fho}} \right)^2 \left(\frac{T_{Fho}}{T_{Feo}} \right)^2 \right) + \frac{h^2 \omega_{ph}^2 \tilde{k}^2}{4m_e^{*2} v_{Fh0}^4} \right] \tilde{k}^2 \cos^2 \theta,$$

$$\tilde{v}_{Fe}''^2 \tilde{k}_x^2 = \left[\tilde{v}_{e,xc}^2 + \left(\frac{m_h^*}{m_e^*} \right)^2 \left(\frac{n_{e0}}{n_{ho}} \right)^{2/3} \frac{3}{5} \left(1 + \frac{5}{12} \pi^2 \tilde{T}_e^2 \left(\frac{m_e^*}{m_h^*} \right)^2 \left(\frac{n_{ho}}{n_{eo}} \right)^{4/3} \right) + \frac{h^2 \omega_{ph}^2 \tilde{k}^2}{4m_h^{*2} v_{Fh0}^4} \left(\frac{m_h^*}{m_e^*} \right)^2 \right] \tilde{k}^2 \cos^2 \theta,$$

$$\tilde{v}_{Fe}''^2 \tilde{k}_x^2 = \left[\tilde{v}_{e,xc}^2 + \left(\frac{m_h^*}{m_e^*} \right)^2 \left(\frac{n_{e0}}{n_{ho}} \right)^{2/3} \frac{3}{5} \left(1 + \frac{5}{12} \pi^2 \tilde{T}_e^2 \left(\frac{m_e^*}{m_h^*} \right)^2 \left(\frac{n_{ho}}{n_{eo}} \right)^{4/3} \right) \right.$$

$$\left. \left\{ 1 + \frac{\tilde{H}^2 \tilde{k}^2 \left(\frac{m_h^*}{m_e^*} \right)^2}{\left(\frac{m_h^*}{m_e^*} \right)^2 \left(\frac{n_{e0}}{n_{ho}} \right)^{2/3} \frac{3}{5} \left(1 + \frac{5}{12} \pi^2 \tilde{T}_e^2 \left(\frac{m_e^*}{m_h^*} \right)^2 \left(\frac{n_{ho}}{n_{eo}} \right)^{4/3} \right)} \right\} \right] \tilde{k}^2 \cos^2 \theta,$$

$$\tilde{v}_{Fe}''^2 \tilde{k}_x^2 = \left[\tilde{v}_{e,xc}^2 + \left(\frac{m_h^*}{m_e^*} \right)^2 \left(\frac{n_{e0}}{n_{ho}} \right)^{2/3} \frac{3}{5} \left(1 + \frac{5}{12} \pi^2 \tilde{T}_e^2 \left(\frac{m_e^*}{m_h^*} \right)^2 \left(\frac{n_{ho}}{n_{eo}} \right)^{4/3} \right) \right.$$

$$\left. \left\{ 1 + \frac{\tilde{H}^2 \tilde{k}^2 \left(\frac{n_{ho}}{n_{eo}} \right)^{2/3}}{\frac{3}{5} \left(1 + \frac{5}{12} \pi^2 \tilde{T}_e^2 \left(\frac{m_e^*}{m_h^*} \right)^2 \left(\frac{n_{ho}}{n_{eo}} \right)^{4/3} \right)} \right\} \right] \tilde{k}^2 \cos^2 \theta.$$

Chapter 4

Numerical Analysis and Discussion

The perturbations in the semiconductor plasma by the electron beam can form various types of waves or modes, such as the Langmuir model, acoustic mode, upper, and lower hybrid modes. The formation of these modes at low temperatures does exist in many materials. An experimental study for several semiconductors like GaN, GaAs, GaSb, and InP shows the formation of these modes. In this thesis, an appropriate theoretical model is used that includes quantum effects such as the Bohm effect, exchange-correlation effect, and Fermi pressure. The effect of electron beam parameters on the propagating wave in electron-hole semiconductor plasma is also investigated.

The study of the propagation and growth rate of L.H.W in electron-hole plasma is of primary interest. This study can be done by introducing $\omega = \omega_r + i\gamma$ in equation (3.126), where ω_r is real angular frequency that describes propagation of wave and γ describes the growth rate. Figure (4.1) shows typical parameters for different semiconductors[16]. Now Applying our theoretical model to GaAs semiconductor with parameters $n_{eo} = 4.7 \times 10^{16} \text{cm}^{-3}$, $\frac{m_e^*}{m_e} = 0.067$, $\frac{m_h^*}{m_e} = 0.5$ and $\epsilon = 12.8$ [47][48][49].

	GaAs	GaSb	GaN
n_{e0}	$4.7 \times 10^{16} \text{ cm}^{-3}$	$1.6 \times 10^{17} \text{ cm}^{-3}$	$1.0 \times 10^{17} - 1.0 \times 10^{20} \text{ cm}^{-3}$
m_e^*	$0.067m_e$	$0.047m_e$	$0.130m_e$
m_h^*	$0.500m_e$	$0.400m_e$	$1.300m_e$
ϵ_L	12.80	15.69	11.30
E_g	1.43 eV	0.78 eV	3.40 eV

Figure 4.1: Typical parameters for different types of semiconductors.

The charge neutrality condition is given as:

$$n_{e0} + n_{b0} = n_{h0}, \quad (4.1)$$

$$\frac{n_{e0}}{n_{h0}} + \frac{n_{b0}}{n_{h0}} = 1, \quad (4.2)$$

$$\alpha + \beta = 1. \quad (4.3)$$

The graphical analysis is done using the above numerical parameters. The graphs given bellow exhibit different behaviors for different numerical values of angle between propagation vector k and x-axis, the streaming speed of the pumped beam electrons (v_0), scaled thermal temperature of the pumped beam electrons T_b , Hole cyclotron frequency ω_{ch} , number density ratio of electron and hole ($\frac{n_{e0}}{n_{h0}}$) and electron and hole temperature (T_e, T_h). Solid lines represent the instability of LH waves, whereas dotted lines describe wave propagation.

Variation of Critical Angle " θ "

The first plot shows the propagation and damping of LHWs for different values of critical angle θ . If the angle between magnetic field $B_0\hat{z}$ and propagation vector $k_x\hat{x}$ is not exactly $\frac{\pi}{2}$. Electrons will move in the direction of $B_0\hat{z}$ because of a smaller Larmor radius to carry out shielding. The holes/ions because of larger Larmor radius cannot do this, that is why we can neglect $k_z\hat{z}$, for holes/ions.

A slight increase in the value of critical angle θ can cause instability spectrum of LH waves to experiences a blue-shift of propagation vector k . The instability sharply grows for a smaller value of θ .

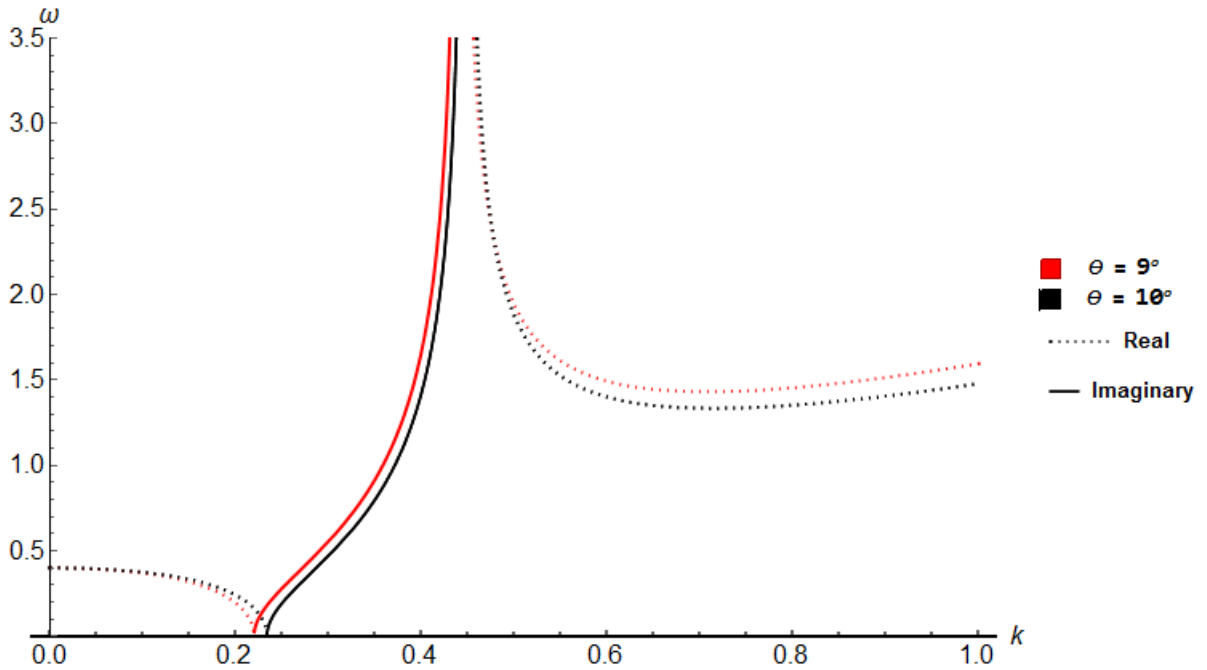


Figure 4.2: Plot between (ω and k) at $\omega_{ch} = 0.4$, $T_b = 0.4$, $T_h = T_e = 0.1$, $v_0 = 1$ and $\alpha = 0.6$. Dotted lines represent real part and Solid lines represent imaginary part at $\theta = 9^\circ, 10^\circ$.

Variation of Streaming Speed " v_0 "

An increase in the speed of electron-beam v_0 will affect the spectrum of the L.H.W significantly. The LHWs spectrum becomes narrow and grows sharply to its maximum value at lower values of k (red-shift in the spectrum). Physically, the high energy beam electrons would give more energy to the system, causing an increase in the speed of systems particles and leads to instability at lower values of k .

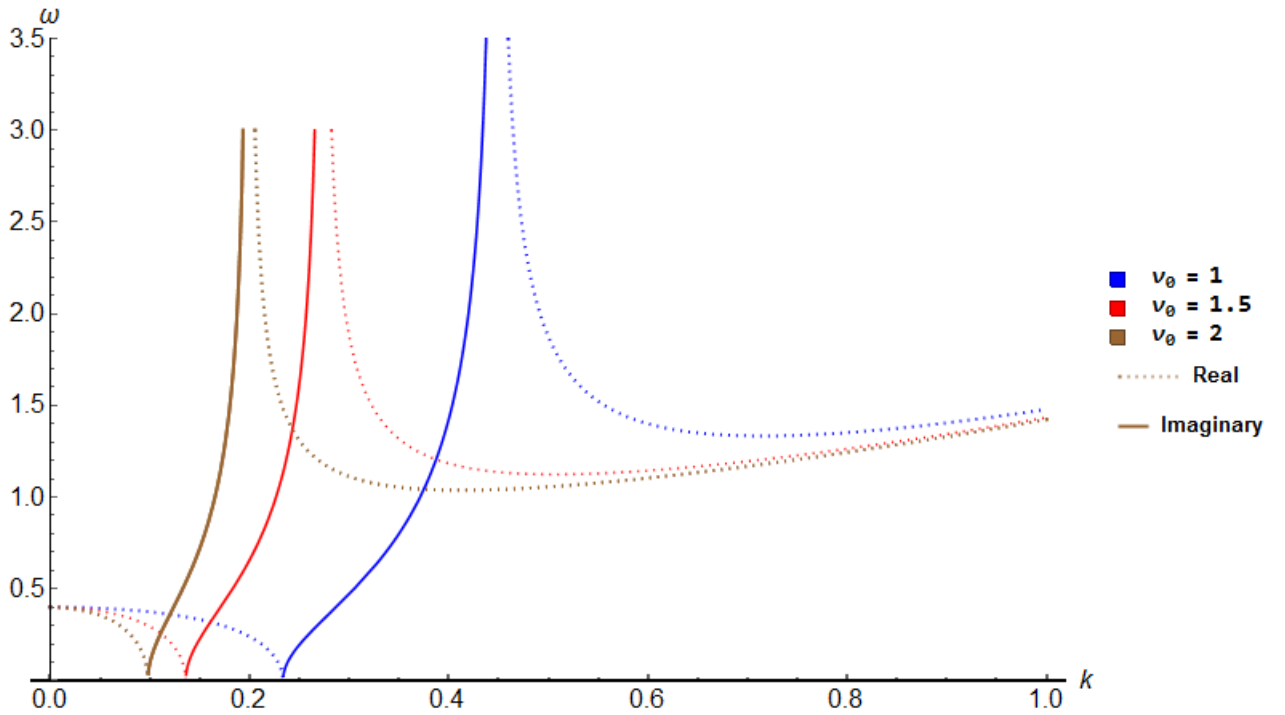


Figure 4.3: Plot between (ω and k) at $\omega_{ch} = 0.4$, $T_b = 0.4$, $T_h = T_e = 0.1$, $\theta = 10^\circ$ and $\alpha = 0.6$. Dotted lines represent real part and Solid lines represent imaginary part at $v_0 = 1, 1.5$ and 2 .

Variation of Beam Temperature " T_b "

An increase in the incoming electron beam temperature T_b will decrease the instability. The spectrum will shift towards higher values of k (blue shift of the spectrum). Physically, high-temperature beam electrons excite a large amount of the high frequency or low wavelength regime, causing a sharp growth of instability in higher values of k . A large number of excited particles will reduce instability.

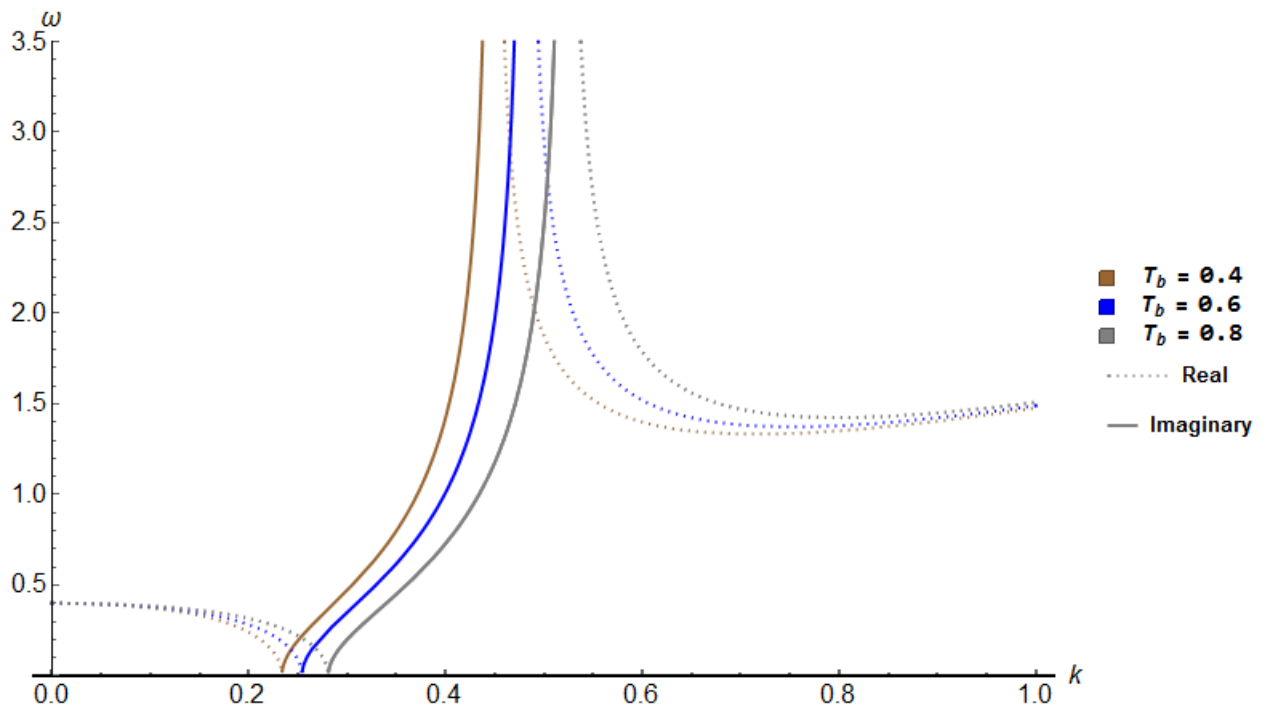


Figure 4.4: Plot between (ω and k) at $\omega_{ch} = 0.4$, $v_0 = 1$, $T_h = T_e = 0.1$, $\theta = 10^\circ$ and $\alpha = 0.6$. Dotted lines represent real part and Solid lines represent imaginary part at $T_b = 0.4, 0.6, 0.8$.

Variation of Hole Cyclotron Frequency " ω_{ch} "

By increasing the values of cyclotron frequency of holes $\omega_{ch} = \frac{eB_0}{m_h^*c}$ will cause a shift in spectrum towards high values of k (blue shift of the wave). The instability spectrum contract for a strong magnetic field and sharply grow at higher values of k . A high magnetic field will confine the particles, this restriction causes more unstable plasma.

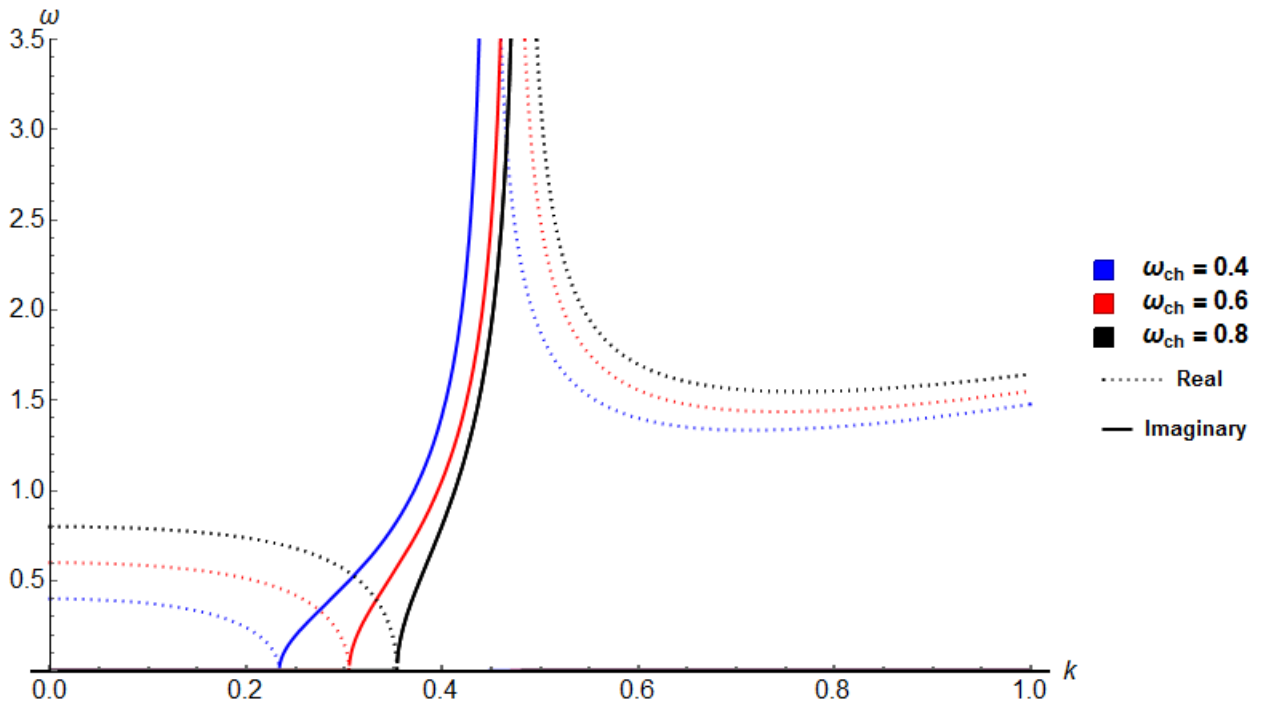


Figure 4.5: Plot between (ω and k) at $T_b = 0.4$, $v_0 = 1$, $T_h = T_e = 0.1$, $\theta = 10^\circ$ and $\alpha = 0.6$. Dotted lines represent real part and Solid lines represent imaginary part at $\omega_{ch} = 0.4, 0.6, 0.8$.

Variation of Electron to Hole Density Ratio " $\alpha = \frac{n_{e0}}{n_{h0}}$ "

Spectrum will become narrow by increasing the value of electron to hole number density $\frac{n_{e0}}{n_{h0}}$. At lower values of k more energetic particles are present which leads to high instability.

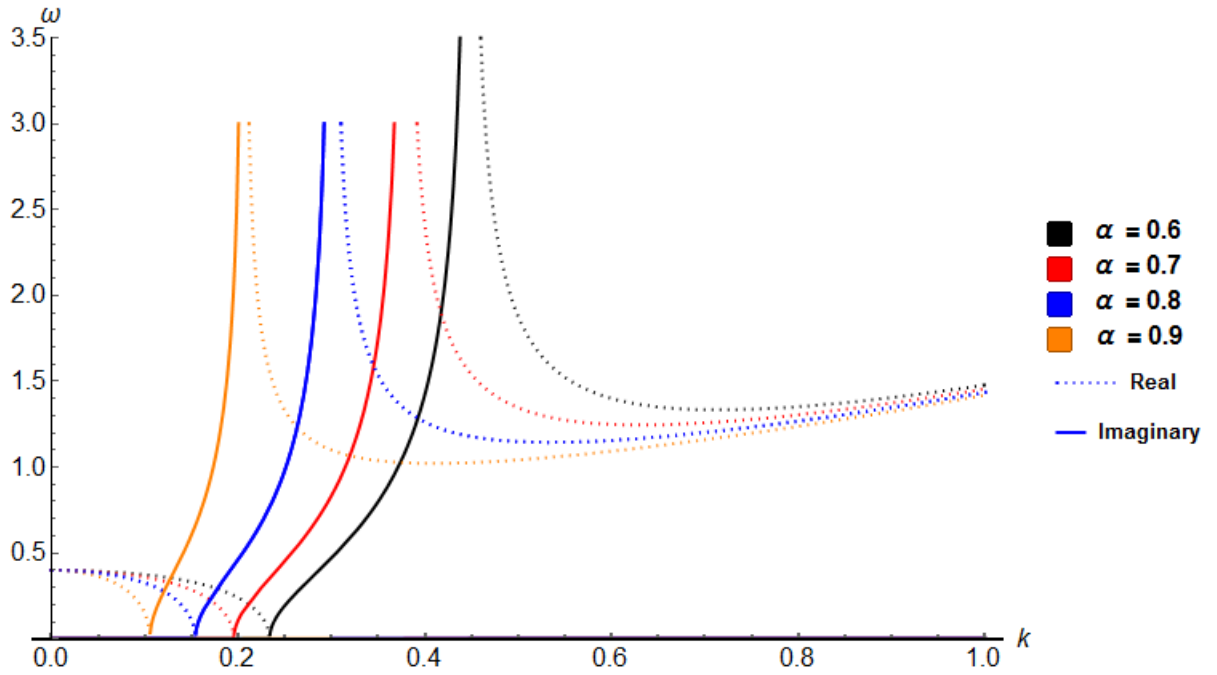


Figure 4.6: Plot between $(\omega$ and $k)$ at $T_b = 0.4$, $v_0 = 1$, $T_h = T_e = 0.1$, $\theta = 10^\circ$ and $\omega_{ch} = 0.4$. Dotted lines represent real part and Solid lines represent imaginary part at $\alpha = 0.6, 0.7, 0.8, 0.9$.

Variation of Scaled Electron and Hole Temperature " T_h, T_e "

An Increase in the scaled electron and hole temperature T_e and T_h will slightly effect the spectrum.

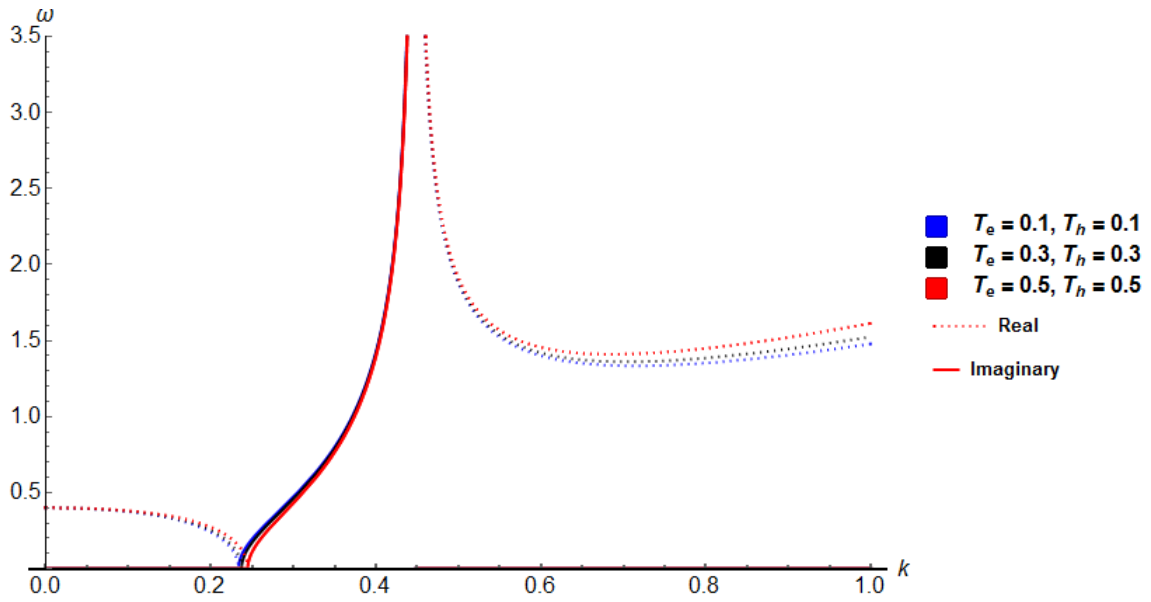


Figure 4.7: Plot between (ω and k) at $T_b = 0.4$, $v_0 = 1$, $\alpha = 0.6$, $\theta = 10^\circ$ and $\omega_{ch} = 0.4$. Dotted lines represent real part and Solid lines represent imaginary part at $T_h = T_e = 0.1, 0.3, 0.5$.

Chapter 5

Conclusion

The theoretical and numerical analysis of propagation of the LH wave in GaAs quantum semiconductors is done in this thesis. The corresponding dispersion relation includes quantum, thermal, and exchange-correlation effects. Variation of certain parameters such as critical angle θ between the wave vector k and the x-axis, number density ratio electron and hole ($\frac{n_{e0}}{n_{h0}}$), scaled electron beam speed ($\frac{v_0}{v_{Fh0}}$), normalized electron beam thermal temperature ($\frac{T_b}{T_{Fh}}$), and normalized hole cyclotron frequency ($\frac{\omega_{ch}}{\omega_{ph}}$), affect the wave propagation and growth rate. An increase in the electron beam speed v_0 and electron to hole density ratio will increase the instability because of the availability of numerous charged particles. The spectrum will become narrow for higher values of v_0 and ($\frac{n_{e0}}{n_{h0}}$). A slight increase in the value of angle θ between the propagation vector of the LH wave and the propagation axis also increases the instability and leads to the blue shift of the wave vector. Increasing the scaled electron beam temperature will decrease the instability due to more excited particles, and the spectrum will shift towards higher values of k . Whereas an increase in the hole cyclotron frequency causes a blue shift in the spectrum and increases the instability. As the influence of the magnetic field increases, the spectrum becomes narrow.

Bibliography

- [1] Fernando Haas. *Quantum plasmas: An hydrodynamic approach*, volume 65. Springer Science & Business Media, 2011.
- [2] Francis F Chen et al. *Introduction to plasma physics and controlled fusion*, volume 1. Springer, 1984.
- [3] Michael C Kelley. *The Earth's ionosphere: plasma physics and electrodynamics*. Academic press, 2009.
- [4] Baumjohann Wolfgang and Treumann Rudolf. *Basic Space Plasma Physics*. World Scientific, 1996.
- [5] G Manfredi and F Haas. Self-consistent fluid model for a quantum electron gas. *Physical Review B*, 64(7):075316, 2001.
- [6] Fernando Haas. An introduction to quantum plasmas. *Brazilian Journal of Physics*, 41(4-6):349–363, 2011.
- [7] PK Shukla and Bengt Eliasson. Colloquium: Nonlinear collective interactions in quantum plasmas with degenerate electron fluids. *Reviews of Modern Physics*, 83(3):885, 2011.
- [8] Giovanni Manfredi. How to model quantum plasmas. *Fields Inst. Commun*, 46:263–287, 2005.

- [9] Claudine Hermann. *Statistical physics: including applications to condensed matter*. Springer Science & Business Media, 2006.
- [10] Sourav Choudhury, Tushar Kanti Das, Malay Kr Ghorui, and Prasanta Chatterjee. The effect of exchange-correlation coefficient in quantum semiconductor plasma in presence of electron-phonon collision frequency. *Physics of Plasmas*, 23(6):062110, 2016.
- [11] P Sumera, A Rasheed, F Areeb, M Siddique, Asif Javed, and M Jamil. Landau quantization effects on hybrid waves in semiconductor plasmas. *The European Physical Journal Plus*, 135(4):356, 2020.
- [12] NS Suryanarayana, Jagjeet Kaur, Vikas Dubey, et al. Study of propagation of ion acoustic waves in argon plasma. *Journal of Modern Physics*, 1(04):281, 2010.
- [13] Giovanni Manfredi and Jérôme Hurst. Solid state plasmas. *Plasma Physics and Controlled Fusion*, 57(5):054004, 2015.
- [14] Mohammad Abdul Wahab. *Solid state physics: structure and properties of materials*. Alpha Science Int'l Ltd., 2005.
- [15] Michael P Marder. *Condensed matter physics*. John Wiley & Sons, 2010.
- [16] RE Burgess. Fluctuations of the numbers of electrons and holes in a semiconductor. *Proceedings of the Physical Society. Section B*, 68(9):661, 1955.
- [17] C David Sherrill. An introduction to hartree-fock molecular orbital theory. *School of Chemistry and Biochemistry Georgia Institute of Technology*, 2000.
- [18] Walter Kohn and Lu Jeu Sham. Self-consistent equations including exchange and correlation effects. *Physical review*, 140(4A):A1133, 1965.

- [19] Nicolas Crouseilles, P-A Hervieux, and Giovanni Manfredi. Quantum hydrodynamic model for the nonlinear electron dynamics in thin metal films. *Physical Review B*, 78(15):155412, 2008.
- [20] Walter Kohn. Density-functional theory for excited states in a quasi-local-density approximation. *Physical Review A*, 34(2):737, 1986.
- [21] AV Andrade-Neto. Dielectric function for free electron gas: Comparison between drude and lindhard models. *Revista Brasileira de Ensino de Física*, 39(2), 2017.
- [22] Kjeld O Jensen, JM Rorison, and Alison B Walker. Temperature-dependent screening and carrier-carrier scattering in heavily doped semiconductors. *Physical Review B*, 48(23):17121, 1993.
- [23] Giancarlo Cappellini, R Del Sole, Lucia Reining, and Friedhelm Bechstedt. Model dielectric function for semiconductors. *Physical Review B*, 47(15):9892, 1993.
- [24] AV Andrade-Neto. Explicit expression for lindhard dielectric function at finite temperature. *arXiv preprint arXiv:1412.5705*, 2014.
- [25] Dietrich Kremp, Manfred Schlanges, and Wolf-Dietrich Kraeft. *Quantum statistics of nonideal plasmas*, volume 25. Springer Science & Business Media, 2006.
- [26] Nicolaas Bloembergen. Laser-induced electric breakdown in solids. *IEEE Journal of Quantum Electronics*, 10(3):375–386, 1974.
- [27] Peter H Yoon. Kinetic instabilities in the solar wind driven by temperature anisotropies. *Reviews of Modern Plasma Physics*, 1(1):4, 2017.
- [28] David H Sharp. Overview of rayleigh-taylor instability. Technical report, Los Alamos National Lab., NM (USA), 1983.

- [29] P Helander and GG Plunk. The universal instability in general geometry. *Physics of Plasmas*, 22(9):090706, 2015.
- [30] Charles T Sebens. Electromagnetism as quantum physics. *Foundations of Physics*, 49(4):365–389, 2019.
- [31] GM Wysin. Quantum theory for dielectric properties of conductors, b. magnetic fields and landau levels, 2011.
- [32] A Rasheed, M Jamil, M Siddique, F Huda, and Y-D Jung. Beam excited acoustic instability in semiconductor quantum plasmas. *Physics of Plasmas*, 21(6):062107, 2014.
- [33] M Jamil, A Rasheed, Ch Rozina, WM Moslem, and M Salimullah. Beam driven upper-hybrid-wave instability in quantized semiconductor plasmas. *Physics of Plasmas*, 21(2):020704, 2014.
- [34] Daniel B Graham, Yu V Khotyaintsev, C Norgren, Andris Vaivads, Mats André, JF Drake, J Egedal, M Zhou, O Le Contel, JM Webster, et al. Universality of lower hybrid waves at earth’s magnetopause. *Journal of Geophysical Research: Space Physics*, 124(11):8727–8760, 2019.
- [35] AL Verdon, Iver H Cairns, DB Melrose, and PA Robinson. Warm electromagnetic lower hybrid wave dispersion relation. *Physics of Plasmas*, 16(5):052105, 2009.
- [36] Prerana Sharma. Modified dispersion properties of lower hybrid wave with exchange correlation potential in ultra-relativistic degenerate plasma. *Physics Letters A*, 382(27):1796–1800, 2018.
- [37] Paul Murray Bellan and Miklos Porkolab. Experimental studies of lower hybrid wave propagation. *The Physics of Fluids*, 19(7):995–1006, 1976.

- [38] King-Lap Wong, Robert Horton, and Masayuki Ono. Current generation by unidirectional lower hybrid waves in the act-1 toroidal device. *Physical Review Letters*, 45(2):117, 1980.
- [39] S Poedts. Kinetic plasma theory (kt-1).
- [40] MA Prakapenia and GV Vereshchagin. Pauli blocking effects in thermalization of relativistic plasma. *arXiv preprint arXiv:2003.07288*, 2020.
- [41] Shabbir A Khan and Michael Bonitz. Quantum hydrodynamics. In *Complex Plasmas*, pages 103–152. Springer, 2014.
- [42] SV Vladimirov and Yu O Tyshetskiy. On description of quantum plasma. *arXiv preprint arXiv:1101.3856*, 2011.
- [43] Peter J Riggs. Reflections on the debroglie–bohm quantum potential. *Erkenntnis*, 68(1):21–39, 2008.
- [44] Michael Bonitz, Zh A Moldabekov, and TS Ramazanov. Quantum hydrodynamics for plasmas—quo vadis? *Physics of Plasmas*, 26(9):090601, 2019.
- [45] Suresh C Sharma, MP Srivastava, M Sugawa, and VK Tripathi. Excitation of lower hybrid waves by a density-modulated electron beam in a plasma cylinder. *Physics of Plasmas*, 5(9):3161–3164, 1998.
- [46] Ved Prakash, Vijayshri, Suresh C Sharma, and Ruby Gupta. Electron beam driven lower hybrid waves in a dusty plasma. *Physics of Plasmas*, 20(5):053701, 2013.
- [47] Arthur N Strahler. Quantitative analysis of watershed geomorphology. *Eos, Transactions American Geophysical Union*, 38(6):913–920, 1957.

- [48] Yunliang Wang and Xiaoxia Lü. Modulational instability of electrostatic acoustic waves in an electron-hole semiconductor quantum plasma. *Physics of Plasmas*, 21(2):022107, 2014.
- [49] ME Yahia, IM Azzouz, and WM Moslem. Quantum effects in electron beam pumped gaas. *Applied Physics Letters*, 103(8):082105, 2013.